Comprehensive Review of Distributed FACTS Control Algorithms for Power Quality Enhancement in Utility Grid With Renewable Energy Penetration.

Chawda, Gajendra Singh; Shaik, Abdul Gafoor; Mahela, Om Prakash; Padmanaban, Sanjeevikumar; Holm-Nielsen, Jens Bo

Published in:
IEEE Access

DOI (link to publication from Publisher):
10.1109/ACCESS.2020.3000931

Publication date:
2020

Document Version
Publisher's PDF, also known as Version of record

Received May 8, 2020, accepted June 3, 2020, date of publication June 8, 2020, date of current version June 19, 2020.

Digital Object Identifier 10.1109/ACCESS.2020.3000931

Comprehensive Review of Distributed FACTS Control Algorithms for Power Quality Enhancement in Utility Grid With Renewable Energy Penetration

GAJENDRA SINGH CHAWDA[1], (Graduate Student Member, IEEE), ABDUL GAFOOR SHAIK[1], (Member, IEEE), OM PRAKASH MAHELA[2], (Member, IEEE), SANJEEVIKUMAR PADMANABAN[3], (Senior Member, IEEE), AND JENS BO HOLM-NIELSEN[3], (Senior Member, IEEE)

[1]Department of Electrical Engineering, IIT Jodhpur, Jodhpur 342037, India
[2]Power System Planning Division, Rajasthan Rajya Vidyut Prasaran Nigam Ltd., Jaipur 302005, India
[3]Department of Energy Technology, Aalborg University, 6700 Aalborg, Denmark

Corresponding author: Gajendra Singh Chawda (chawda.1@iitj.ac.in)

This project was carried out under the Project No. 19-MG04AAU, Danida Mobility Grant, responsible for the Ministry of Foreign Affairs of Denmark (MFA), Act 7 on Denmark's International Development Cooperation and Visvesvaraya Ph.D. Scheme, MeitY, India, under Project AKT/2014/0030.

ABSTRACT Rapid industrialization and its automation on the globe demands increased generation of electrical energy with more reliability and quality. Renewable energy (RE) sources are considered as a green form of energy and extensively used as an alternative source of energy for conventional energy sources to meet the increased demand for electrical power. However, these sources, when integrated to the utility grid, pose challenges in maintaining the power quality (PQ) and stability of the power system network. This is due to the unpredictable and variable nature of generation by these sources. The distributed flexible AC transmission system (DFACTS) devices such as distributed static compensator (DSTATCOM) and dynamic voltage restorer (DVR) play an active role in mitigating PQ issues associated with RE penetration. The performance of DFACTS devices is mostly dependent on the type of control algorithms employed for switching of these devices. This paper presents a comprehensive review of various conventional and adaptive algorithms used to control DFACTS devices for improvement of power quality in utility grids with RE penetration. This review intends to provide a summary of the design, experimental hardware, performance and feasibility aspects of these algorithms reported in the literature. More than 170 research publications are critically reviewed, classified, and listed for quick reference for the advantage of engineers and academician working in this area.

INDEX TERMS Adaptive control algorithm, conventional control algorithm, DFACTS device, modern utility grid, power quality, renewable energy source.

ABBREVIATIONS

3P4W	Three phase four wire
3P3W	Three phase three wire
ABT	Admittance based theory
ACA	Adaptive control algorithm
ADALINE	Adaptive linear element theory
ALMS	Adaptive least mean square
ANF	Adaptive notch filter
ANFIS	Adaptive neuro-fuzzy inference system
ARLS	Adaptive recursive least square
CCA	Conventional control algorithm
DFACTS	Distributed flexible AC transmission system
DSP	Digital signal processing
DSSSC	Distributed static synchronous series compensator
DSSC	Distributed static series compensator
DSTATCOM	Distributed static compensator
DSVC	Distributed static var compensator

The associate editor coordinating the review of this manuscript and approving it for publication was Guangya Yang.

DTCSC	Distributed thyristor controlled series compensator
DVR	Dynamic voltage restorer
EPLL	Enhanced phase-locked loop
FC	Fuel cell
FLC	Fuzzy logic controller
FPGA	Field programmable gate array
HCC	Hysteresis current controller
ICCT	Indirect current control theory
IPQC	Interline power quality compensator
IRPT	Instantaneous reactive power theory
LMF	Least mean fourth
LMS	Least mean square
LPF	Low pass filter
PCC	Point of common coupling
PLL	Phase locked loop
PQ	Power quality
PMSG	Permanent magnetic synchronous generator
PWM	Pulse width modulation
RE	Renewable energy
RES	Renewable energy sources
RLS	Recursive least square
RSGA	Reference signal generation algorithm
SAPF	Shunt active power filter
SEIG	Self-excited induction generator
SMC	Sliding mode controller
SOGI	Second order generalized integrator
SPV	Solar photo-voltaic
SPWM	Sinusoidal pulse width modulation
SRFT	Synchronous reference frame theory
SyRG	Synchronous reluctance generator
THD	Total harmonic distortion
TDD	Total demand distortion
UPQC	Unified power quality conditioner
VFFRLS	Variable forgetting factor RLS
VSC	Voltage source converter
VSLMS	Variable step LMS
WES	Wind energy source

NOMENCLATURE

v_{sab}, v_{sbc}	Sensed voltages at PCC
i^*_{pabc}, i^*_{qabc}	Reference active and reactive currents
i_{sabc}, i^*_{sabc}	Sensed and reference grid currents
W_{RES}	Feed forward weight component of RES
u_{pabc}, u_{qabc}	Active and reactive unit templates
v_t, v_{tn}	Sensed and reference terminal voltages
v_{dc}, v^*_{dc}	Sensed and reference voltage of dc link
v_{de}, v_{te}	Voltage errors of PI controller
W_{pabc}, W_{qabc}	Active and reactive weight components of load current
Z_g	Impedance of grid/source
L_f, R_f	Interfacing inductor and resistor
C_{dc}, C_f	DC link and ripple filter capacitors
τ_p, τ_q	Active and reactive adaptive constants
W_{Lpa}, W_{Lqa}	Average active and reactive weights
k_{id}, k_{iq}	Integral constant of PI controller
k_{pd}, k_{pq}	Proportional constant of PI controller
B_{qt}, G_{pt}	Susceptance and conductance
$j(n), \lambda$	Cost function and forgetting factor
$k(n), P(n)$	Kalman gain and correlation matrix
I_{SC}, I_L	Maximum short circuit current and load at PCC

I. INTRODUCTION

The increased demand for electrical power, the requirement of environmental conservation and depletion of fossil fuel reserves have forced the utilities to increase the penetration level of RE into the utility grid [1], [2]. Renewable power can reduce power losses, mitigate environmental pollution, defer or eliminate system upgrades, reduce operating costs, and improve voltage profile due to their nature and penetration at distribution level [3]. The share of RES in total primary energy supply would rise from 14% in 2015 to 63% in 2050 [4]. The high penetration level of renewable energy (RE) sources into the utility grid lead to PQ challenges and deteriorate the quality of electrical power significantly [5]. PQ issues associated with the grid integration of RE sources include fluctuations in voltage, reactive power flow, harmonics, excessive neutral current, etc. [6]–[9]. The other important issues associated with RE placement, sizing and voltage ride-through in distribution systems reported in [10], [11]. Research work to resolve the issues of power quality associated with WES, SPV, and FC is investigated using simulation studies [12] and hardware approach [13]. This work further also investigated the enhancement of stability of the utility network in the presence of RE. The development of DFACTS devices used in the distribution network to improve the PQ has also resulted in the increased RE penetration levels in the grid [14], [15]. The studies also revealed that PQ mitigation could be achieved using distribution static compensator controlled by synchronous reference frame theory [16]. This is also validated by the use of real-time digital simulation (RTDS). The DFACTS devices including, DSTATCOM, DVR, and UPQC were found to be effective in mitigating PQ issues such as harmonics and load unbalancing [17], [18]. These devices also help to maintain voltage regulation [19], [20]. However, the performance of DFACTS technologies is largely dependent on the implemented control algorithm [21]. These control algorithms may be conventional and adaptive in nature [22]. The conventional control algorithms are implemented using instantaneous symmetrical component theory (ISCT), instantaneous reactive power theory (IRPT), synchronous reference frame theory (SRFT), etc. [23]–[28]. The SRFT control algorithm is the widely used conventional control method for PQ improvement. The performance of these algorithms is not satisfactory due to the use of the inbuilt phase-locked loop (PLL). An important feature desired in the smart grid control and operation is the fast response of control algorithm. Further, it is also desired that these control algorithms track the changes associated with RE penetration and the dynamics of the loads accurately. These can not be

TABLE 1. Symptoms, causes, impacts and solution of PQ disturbances in 3P3W and 3P4W utility network [1]–[65].

PQ Disturbances	Details
Voltage sag or dip	**Description**: The RMS voltage level decreases between 10-90% of nominal voltage for ½-cycle to 1-minute. **Symptoms**: Memory loss and data errors, equipment shutdown, decreased equipment life and flickering lights. **Causes**: Faults on the 3P3W or 3P4W utility system, start-up of large motors, inductive loading and switching on the large loads. **Impacts**: Malfunction of embedded based equipment, personal computers, programmable logic controls, and tripping of sensitive equipment. **Solution**: DVR, DSSC, static transfer switch.
Very short Interruptions	**Description**: Complete loss of electrical supply for a few milliseconds to 1 second. **Symptoms**: Decreased equipment life and Flickering lights. **Causes**: Automatic opening and reclosing of protection devices of 3P3W and 3P4W utility network and life of sensitive equipment. **Impacts**: Tripping of sensitive equipment and electromechanical relays and malfunctioning. **Solution**: Machine-Generator set, DSSSC, DVR, static transfer switch.
Long Interruptions	**Description**: Complete loss of electrical supply for a duration greater than 1-2 sec. **Symptoms**: Loss of supply to customer equipment and computer shutdowns. **Causes**: Equipment failure, trees, fire, vehicles striking to lines or poles, failure of protection device and circuit breaker tripping. **Impacts**: Equipment shutdown and sudden damaging occurred in sensitive equipment. **Solution**: DVR, UPQC, Machine-Generator set, DSSSC.
Voltage spike	**Description**: Abrupt rise or fall of the voltage value for a short duration ranging from several microseconds to few milliseconds. **Symptoms**: Flickering lights, data loss and interference. **Causes**: Lightning, lagging PF, capacitor switching and phase faults. **Impacts**: Destruction of electronic components, tripping of sensitive equipment, damage to insulation and winding. **Solution**: DVR, DSSSC, UPQC.
Voltage swell	**Description**: The RMS voltage level increases to 110%-180% of nominal voltage, at the power frequency for duration of ½-cycle to 1-minute. **Symptoms**: Memory loss and data errors, equipment shutdown, decreased equipment life and flickering lights. **Causes**: Switch ON and switch OFF heavy loads, transformers regulation is affected during off-peak hours. **Impacts**: Loss of efficiency in electric rotating machines. **Solution**: DSVC, DSTATCOM, DVR, UPQC.
Harmonic Distortion	**Description**: Superposition of various sine waves into distorted waveform with different phase, magnitudes and multiples of power frequency. **Symptoms**: Electrical equipment/wiring overheated, the decreased performance of the equipment, improper operation of relays. **Causes**: Arc furnaces, welding machines, weak AC grid, non-linear loads, integration of renewable energy sources and rectifier. **Impacts**: Increase neutral current, nuisance tripping of thermal protections, mal-operation of sensitive equipment, overheating. **Solution**: Active and passive filters, multi-pulse configuration.
Voltage Fluctuation	**Description**: Voltage oscillations with amplitude modulation at a frequency of 0 to 30 Hz. **Symptoms**: Dim or bright lights, speed variation of dynamic loads, overheating of equipment and reduced life of the equipment. **Causes**: AC drives, unbalanced loads, inter-harmonic current components, welding and arc furnaces. **Impacts**: Flickering of lighting, fluorescent and incandescent lamps. **Solution**: DSVC, DSTATCOM, DVR, UPQC.
Voltage Unbalance	**Description**: Unevenness in voltage magnitude with varying phase angle. **Symptoms**: Overheating of equipment, reduced efficiency and speed variation in motors. **Causes**: Large 1-phase loads mainly due to the furnaces load, traction load, unbalanced loads and location of grid-tied RESs. **Impacts**: 3-phase induction machines, overheating in motors and life of the equipment. **Solution**: DSVC, DSTATCOM, DVR, UPQC.
Over voltage	**Description**: A condition in which the voltage value exceeds the rated design limit. **Symptoms**: Dim or bright lights, equipment shut down, over heatings of equipment and reduced efficiency. **Causes**: Unbalanced and balanced load switching, capacitor switching and system voltage regulation. **Impacts**: Overheating in motors, mal-operation of sensitive equipment, relays and life of the equipment. **Solution**: DSVC, DSTATCOM, DVR, UPQC.
Power frequency Variation	**Description**: Any deviation in the fundamental frequency. **Symptoms**: Dim or bright light, heating, reduced efficiency and motors run slower. **Causes**: Usually caused by failure of the generator, extreme loading conditions **Impacts**: Logic-based systems may fail and massive power failure in the grid. **Solution**: DSVC, DSTATCOM, DVR, UPQC.
Under voltage	**Description**: A condition in which the voltage reduces below the rated value of the power system equipment. **Symptoms**: Dim or bright lights, equipment shut down, reduced efficiency, distortion and malfunctioning. **Causes**: Heavy network loading, loss of generation, power factor variation, lack of Var support. **Impacts**: All equipment without backup supply facilities shut down in this condition. **Solution**: DSSSC, DSTATCOM, DVR, UPQC.
Other possible solution	Proper earthing of equipment, energy storage systems, network equipment and design, online or hybrid UPS [17].

achieved efficiently by the use of conventional control methods. Hence, the researchers have focused on the development of adaptive algorithms for the control of smart utility grid, which might provide an effective solution for PQ and stability challenges. These algorithms also provide the possibility of high RE penetration level of in the 3P3W and the 3P4W utility grid. These algorithms include Adaline, ALMS, and ARLS based algorithms [29]–[34]. These algorithm functions using the principle of continuously updating the weight component according to the system data. The attractive features of these algorithms include simple architecture, simplified calculation and fast convergence with a negligible steady-state error. These control algorithms have been successfully validated in the hardware framework using R&D controllers such as DSP, FPGA and dSPACE [35], [36].

This paper presents a comprehensive focused on the performance of algorithms used for the control of DFACTS devices to improve power quality in 3P3W and 3P4W utility grid with RE penetration, which were validated with hardware framework. More than 170 research publications [1-176] have been reviewed critically and presented in seven sections of this paper. Section 1 in the introduction and introduces the general aspects of power quality and DFACTS devices. Section 2 covers power quality issues and international guidelines for their mitigation. Section 3 presents the use of DFACTS devices in the area of PQ improvement in utility grid with RE penetration. Experimental implementation of DFACTS devices in 3P3W and 3P4W utility grid with RE penetration is described in Section 4. Section 5 details the principles and block diagrams of various control algorithms used for the DFACTS. Key findings and recommendation for future research work are presented in Sections 6. Finally, the conclusions are drawn in Section 7.

II. POWER QUALITY

In the healthy grid, power quality is referred to the level of customer satisfaction in terms of uninterrupted power supply and maintaining voltage, current and frequency within the permissible limits defined in grid codes [37]. The deviation of these quantities from the permissible range might result in mal-operation and failure of utility and consumer equipment. RE penetration into the utility grid would further deteriorate the quality of power due to the unpredictable output of the RE sources and converters used for their interfacing with the grid [38], [39]. Hence, IEEE has led down the guidelines in terms of PQ, which is computed based on voltage fluctuations, flickers, and frequency distortion in the utility grid with RE penetration [40]. These limit the penetration

TABLE 2. Important International standards for power quality.

Standards	Guidelines	Ref.
929-2000	Guidelines for compatible operation of grid tied-SPV.	[40]
1159	Guidelines for monitoring of electrical PQ.	[42]
519-1992	Guidelines on voltage, current harmonic levels.	[45]
P1547	Guidelines for grid-tied RES with the power system.	[46]
519-2014	Guidelines on updated voltage, current harmonic levels and short time harmonic measurements.	[47]
61000-4-7	Guidelines on harmonics and inter-harmonics measurement and instrumentation.	[47]
61000-4-15	Guidelines for testing and measurement methods-flicker meter—functional and design specifications.	[47]
61000-4-30	Guidelines for PQ measurement methods.	[47]
P1409	Guidelines for PQ improvement in utility network using custom power technologies.	[48]

level of RE sources into the distribution grid. Therefore, PQ mitigation is a major concern for electric smart grids [41]. The commonly observed PQ disturbances, their symptoms, causes of these disturbances, their impacts on equipment and possible mitigation approaches are detailed in Table 1. The data included in Table 1, are selected from the books and research articles cited in this review paper. Further, appropriate PQ mitigation techniques are discussed in this Table. This will help the readers to select the appropriate DFACTS device for mitigation of a specific PQ disturbance. Also, the possible alternate solutions for PQ mitigation is also included in this Table which would give the basic idea for minimization of the PQ disturbances. This would be helpful when DFACTS devices are not present in the system.

A. INTERNATIONAL STANDARDS OF POWER QUALITY

International bodies such as Institute of Electrical and Electronics Engineers (IEEE), European Committee for Electrotechnical Standardization (CENELEC) and International Electrotechnical Commission (IEC) are continuously coordinating with each other to standardize the PQ at grid level [42]. These organizations provide various international standards on PQ, which help to regulate the PQ with and without RE penetration. The guidelines for power loss analysis with SPV penetration proposed in [43]. The IEEE standard 519-1992 helps to understand harmonics in power system network [44], [45]. IEEE-P1547 standard states that voltage fluctuations must be less than ±5% and the amount of DC content must be less than 0.5% of total output current at the PCC [46]. The harmonics voltage and current limits for different voltage levels are updated in IEEE standard 519-2014 [47]. This updated standard significantly focused on harmonic measurements and introduced the statistical evaluation in brief and short time-harmonic measurements. It can be perceived from IEEE standard 519-2014, that the voltage distortion level decreases with an increase in voltage level and current harmonics limits depend on the short circuit strength of the system. The relevant IEEE standards related to PQ and RE penetration into the utility grid are presented in Table 2.

III. DFACTS DEVICES

The DFATCS devices are the flexible AC transmission system (FACTS) devices used in the distribution grid to control line impedance, phase angle, current harmonics, voltage harmonics, voltage magnitude and unbalance loading to maintain power quality. In [49], [50], a new concept of DFACTS is recommended, which is a promising economical solution to PQDs in a utility grid-tied with RE sources. It also provides many advantages as they are small in size, less in cost, and easy for implementation compared to conventional FACTS devices. They are found to be effective in the control of phase angle and line impedance [51], [52]. The DFACTS devices are efficient in the enhancement of PQ in the utility grid with RE penetration [53]. Performance comparison of DFACTS devices for PQ improvement has been presented in Table 3. Performance of the DFACTS devices for PQ mitigation will depend on the different attributes which are included and discussed in this Table. These attributes of DFACTS devices are beneficial to evaluate performance level in hardware design.

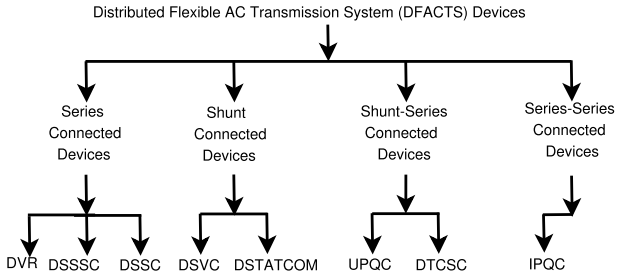

FIGURE 1. Classification of DFACTS devices.

TABLE 3. Performance comparison of DFACTS devices.

Attributes	DFACTS devices for PQ improvement			
	IPQC	DSSSC	DSTATCOM	UPQC
Reactive power compensation	Good	Poor	Best	Best
Harmonic suppression	Adjustable	Adjustable	Adjustable	Adjustable
Resonance	No	May exist	No	No
Load balancing	Good	Good	Best	Good
Transient stability	Good	Good	Better	Best
Steady state stability	Good	Good	Better	Best
Voltage control	Good	Good	Best	Best
Power rating of converter	Small	High	High	Small
Number of switches	9-12	6	6	12
Overall cost	Medium	Low	Low	Medium
Performance level in hardware design	Good	Good	Better	Best

The main advantages of DFACTS for PQ improvement in the utility grid with RE penetration as follows [54],

- Enhanced utilization of existing utility grid.
- Increased flexibility and power flow control in a utility grid with RE penetration.
- Enhancement of transient and dynamic stability limit of the utility grid.
- Increased system reliability and security.
- Environmental friendly.
- Increased quality of power supply.

The details related to various DFACTS devices are also provided in the below subsection.

A. TYPES OF DFACTS DEVICES

The DFACTS devices can be classified into series-connected, shunt connected, shunt-series connected, and series series connected based on interconnection with utility grid as shown in Fig 1.

1) SERIES DFACTS DEVICES

These compensators are connected in series with the utility grid. They may have mutable impedance like a capacitor and reactor. Series compensators work on the principle of injecting voltage in series with grid voltage thereby controlling the real power flow in the utility network. This minimizes real and reactive power loss in the distribution network [55], [56]. These devices can also be utilized to limit the short circuit current, eliminating the subsynchronous resonance (SSR) and damping power oscillations [57]. Commonly used series-connected DFACTS devices include DSSC, DSSSC, DVR etc.

2) SHUNT DFACTS DEVICES

A shunt compensator is a VSC connected in parallel with the utility grid [58]. It may have mutable impedance and source. Shunt compensators work on the principle of injecting current in shunt with grid voltage, thereby allowing power flows by enhancing the voltage profile in the utility network. These devices help in maintaining power factor, balancing the load, mitigating reactive power, reducing harmonics, and providing uninterrupted power [56], [59]. Commonly used shunt connected DFACTS devices include DSTATCOM, DSVC, etc.

3) SHUNT-SERIES DFACTS DEVICES

This compensator provides both shunt and series compensation. These are controlled in a co-equal manner using series and shunt elements. In this compensator, shunt component of the compensator inject current, and the series component of the compensator injects voltage in the utility grid. The active and reactive power exchange between these compensators through the dc-link capacitor presented in [60]. These are found to be effective in improving system stability and mitigating PQ issues with RE penetration [61], [62]. Various shunt-series DFACTS devices include UPQC, DTCSC, etc.

4) SERIES-SERIES DFACTS DEVICES

Interline power quality compensator (IPQC) is widely used active and reactive power compensator in utility grid-tied with RE sources. It consists of two branches (inductive and capacitive), which help to control active and reactive power independently by adjusting the phase shifter or branch impedance. The IPQC can regulate power flow in both the direction and minimizes short circuit current, to allow active power flow control in utility network [60], [63]. Combined DFACTS devices have considerable flexibility and hence are more complex and difficult to control.

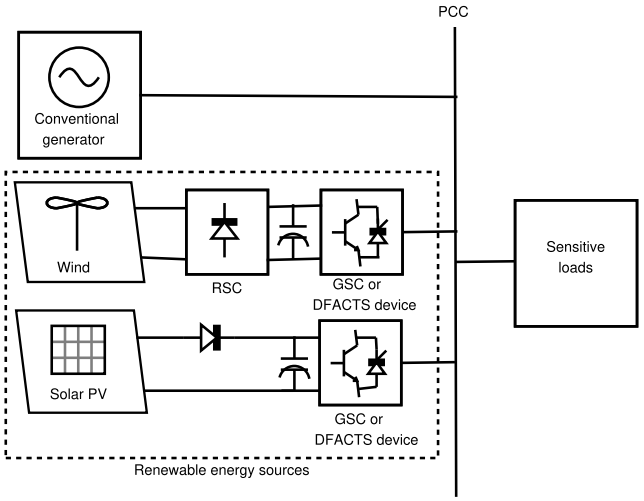

FIGURE 2. Block diagram of PQ mitigation in grid tied RE source.

IV. HARDWARE ARCHITECTURES OF MODERN UTILITY GRID

Block diagram of the new utility network with sensitive load, power quality mitigation device and RE sources at PCC is illustrated in Fig 2. Wind Energy source and Solar-PV have been considered as a renewable energy source, which is connected at the point of common coupling (PCC) through grid side converter (GSC) with the conventional generator. These grid side converters are also termed as DFACTS devices and controlled with appropriate control algorithms. These algorithms are helping to increase the output efficiency of the RE sources. The sensitive loads also connected at PCC, which is considered as a distribution load.

The RE penetration with digital control of DFACTS devices is the main feature of the modern utility grid [64] and requirements for updating and modifying the benchmarks for modern grids are detailed in [65]. The modern architecture of the utility grid can be classified into modern three-phase three-wire (3P3W) and three-phase four-wire (3P4W). The modern 3P3W utility system is employed for balanced three-phase loads, i.e., induction motor load. The major challenge associated with this system includes lack of return path for unbalanced currents which would lead to the unbalanced supply voltage. The architecture of the modern 3P4W utility grid also provides a choice of connecting single-phase loads. In the case of unbalance, neutral wire provides a path for neutral current circulation. The major challenges associated with the modern grid include excessive neutral current, harmonics, and voltage regulation. DFACTS devices help to mitigate power quality issues and allow high RE penetration in modern utility grids. feasibility of different topologies of modern utility grids, based on their performance, with various RE sources, are provided in Table 4. It has been perceived from Table 4 that, one type of RE source integrated with 3P3W or 3P4W utility network is feasible and involves less computational complexity in both the RES side and grid side

TABLE 4. Feasibility of modern 3P3W and 3P4W utility grid with various RES.

RES	Utility network type		RES side control			Grid side control		Feasibility
	3P3W	3P4W	P&O	I&C	ACA	CCA	ACA	
SPV	2	2	2	2	2	2	2	1
Wind	2	2	2	2	2	2	2	1
FC	2	2	2	2	2	3	2	1
SPV+ Wind	3	3	2	2	3	3	2	1
SPV +FC	3	3	3	3	3	3	2	1
SPV+ Wind +FC	3	3	3	3	3	3	3	1

*feasible = 1, applicable = 2, applicable with complexity = 3
P & O = perturbation and observation, I & C = incremental and conductance

controls. However, complexity will be increased when hybrid RE penetration (two or more types of RE sources) is available. This is observed due to the requirement of synchronized control for all converters in the presence of hybrid RE sources. Hence, there is the trade-off between single and hybrid RE sources in the utility grid. On the one hand, the single RE source in the utility grid has better performance than the hybrid RE sources in terms of less complexity, and on other hands, the output power performance of hybrid RE penetration would be the better option for meeting load demands.

A. MODERN 3P3W UTILITY GRID

The experimental architecture for RE sources integrated to 3P3W utility grid with DFACTS device is depicted in Fig 3. The modern 3P3W utility grid is realized from a 50Hz three-phase AC grid with RE source (ETS600 X 17DPVF) supplying power to the nonlinear/sensitive loads. Meanwhile, power quality is improved by DFACTS (SKM50GB123) device. The switching signals are provided by control algorithm via dSPACE 1103 or 1104. The voltage and current signals are sensed by LEM LV-25P and LEM LA-55P hall-effect based sensors. The optical isolation is provided by optocoupler 6N136. The 3P3W hardware framework reported in the literature includes grid-integrated DFIG in [66] for power quality improvement. Single-stage SPV-DSTATCOM based configuration for power quality improvement have been presented in [67]–[71]. This configuration has also been utilized for the multi-functional operation of DSTATCOM in [72], [73] to show system capabilities. A three-leg DSTATCOM has been employed for PQ mitigation under varying solar intensity levels in [74] and sundry system perturbation in [75]. This also has been used to supply active power to the utility grid and loads in [76]. The grid interfaced two-stage PV system with DSTATCOM has been utilized for power quality mitigation in [77], [78]. Photo-voltaic RE source integrated into hybrid DSTATCOM for PQ improvement is presented in [79]. A hybrid PV-wind-battery system with three legs DSTATCOM has been used in [80] for optimum power flow between the micro-grid and the distribution grid. These investigations demonstrated the multi-functional capabilities of DFACTS devices with RE penetration in the 3P3W utility system.

B. MODERN 3P4W UTILITY GRID

The experimental architecture for RE penetration into 3P4W utility grid with DFACTS device is depicted in Fig 3 with highlighted fourth wire. This highlighted fourth wire (neutral wire) would help to provide more clarity and difference between Experimental architecture for RE penetration into 3P3W and 3P4W utility grid with DFACTS. The modern 3P4W utility grid realized using a 50Hz three-phase AC grid with RE source (ETS600 X 17DPVF) supplying power to the nonlinear load. Meanwhile, power quality is improved by DFACTS (SKM100GB128DN) device. The control algorithm provides the switching signals via dSPACE 1202 micro lab box. ABB-EM10BB and EL50P1BB hall-effect based sensors sense the voltage and current signals. The optical isolation is provided by optocoupler 6N136. In 3P4W utility grid, the neutral conductor of the load and fourth leg of DFACTS device is connected through the neutral wire. This fourth leg of DFACTS device, with coupling inductor, is also utilized for compensation of excessive neutral current. The 3P4W hardware framework reported in the literature includes the design of an SPV system with four-leg DSTATCOM [81], [82]. The self-excited induction generator with adaptive stator current compensator for voltage and speed control is presented in [83]. The single-stage SPV with DSTATCOM is used in [84] for power quality improvement under unbalanced loads. Shunt Active Power Filter (SAPF) for mitigating the neutral-point oscillation has been presented in [85]. A 4-leg DSTATCOM has been employed to limit fault current [86], to compensate the neutral current [87], mitigate unbalanced load variations [88] and excessive neutral current [89], [90]. These investigations demonstrated the multi-functional capabilities of DFACTS devices with RE penetration in the 3P4W utility system.

As a conclusion of section IV, the performance of modern utility grid in terms of PQ mitigation largely depends on the type of load, RES, strength of AC grid and power quality mitigation methodology (selection of DFACTS device and its control algorithm) [53]. The significant difference of selection of DFACTS devices and its control algorithms for 3P3W and 3P4W modern utility grid is highlighted below:

- The 3P3W modern utility grid requires 3-leg Insulated Gate Bipolar Transistor (IGBT) switch, which is based on the specific application (i.e. shunt compensation or series compensation).
- The 3P4W modern utility grid requires fourth-leg of IGBT based thyristor for alleviating the neutral current.
- To control the fourth transistor of the 3P4W modern utility grid extra PWM is required which is generated by the control algorithm by using fourth wire of the system. The control algorithm computes extra PWM for fourth-leg of the switch by comparing sensed (actual) neutral current signal and reference neutral current signal. The recommended features of these algorithms include robustness, speed and adaption to the system changes based on the current information related to load and RE sources.

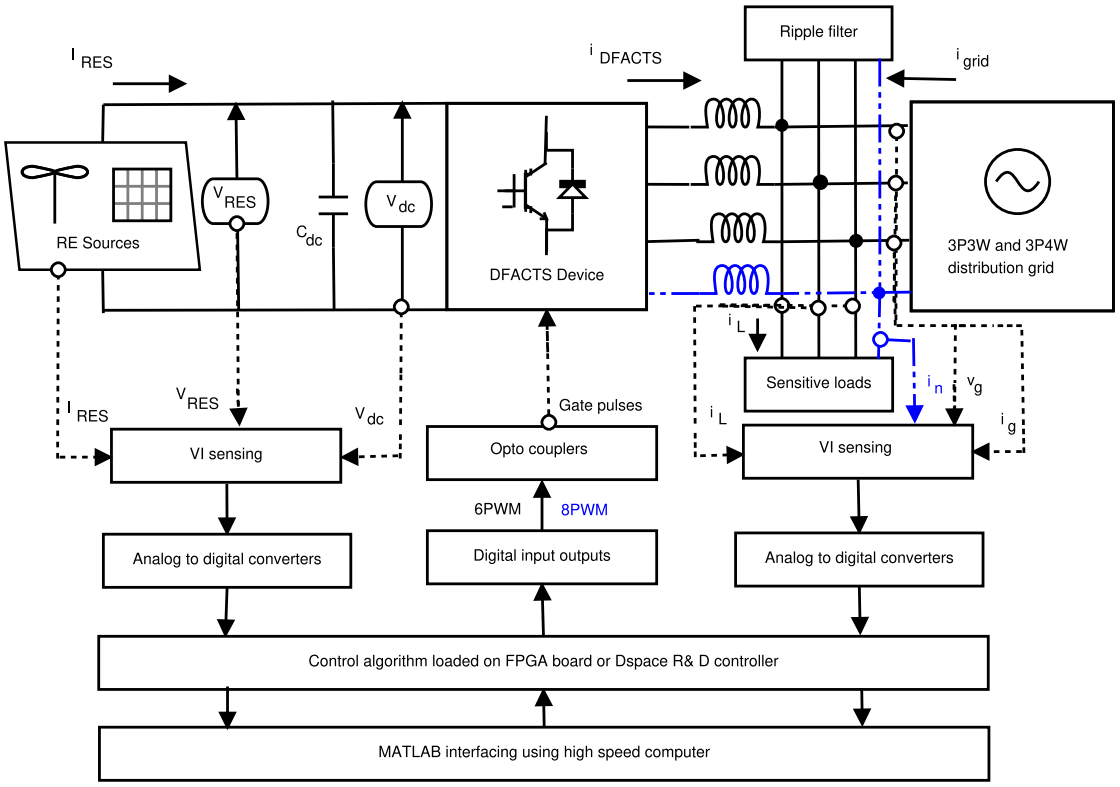

FIGURE 3. Experimental architecture for RE penetration in to 3P3W and 3P4W utility grid with DFACTS.

V. THE EXISTING CONTROL ALGORITHMS

Various control algorithms, proposed to estimate reference signals, which in turn used to control DFACTS devices are broadly classified into two categories, namely frequency-domain (FD) and time-domain (TD) algorithms. The performance of these algorithms is graded based on how fast and accurate reference signals are generated. The frequency-domain based algorithms include recursive discrete Fourier transform (DFT), fast Fourier transform (FFT) and miscellaneous FD based algorithms. These algorithms for power quality mitigation studies are not often used due to their inaccuracy, as reported in [91]. The TD based control algorithms found to be suitable for power quality mitigation [92]. These algorithms are sub-classified into conventional control and adaptive control algorithms. The existing conventional control algorithm (CCA) are based on Clark transformation of voltage and current signals. Adaptive control algorithm (ACA) are based on error minimization and weight updation of voltage and current signals. Fig 4 presents the general classification of various control algorithms.

A general hardware block diagram of these control algorithms is depicted in Fig 5. Various functional blocks of control algorithm include sensors, signal conditioning unit, and interface with the high-speed computer through FPGA or dSPACE controller. The high-speed computer processes various inputs, including the system data and output switching signals to DFACTS devices via optocoupler and buffer circuit.

A. CONVENTIONAL CONTROL ALGORITHMS

Conventional control algorithms work on the concept of 3-phase to 2-phase and 2-phase to 3-phase transformation of voltage and current signals with phase-locked loop circuit for the estimation of reference gate signals required to drive the DFACTS devices [93]. The design process involved for designing of conventional control algorithm is explain in below subsection.

1) DESIGN OF CONVENTIONAL CONTROL ALGORITHM

Various steps involved in designing of conventional control algorithms are detailed below. Standard notation and nomenclature are used based on the research articles cited in this review.

- **Estimation of in-phase and quadrature unit templates**: The ac terminal voltage v_t is determine using the three-phase source/grid voltages (v_{sa}, v_{sb}, v_{sc}) as,

$$v_t = \sqrt{2/3(v_{sa}^2 + v_{sb}^2 + v_{sc}^2)} \tag{1}$$

Three-phase in-phase (active) unit vector templates (u_{pa}, u_{pb}, u_{pc}) can be written as,

$$u_{pa} = v_{sa}/v_t, \quad u_{pb} = v_{sb}/v_t, \; u_{pc} = v_{sc}/v_t \tag{2}$$

Three-phase quadrature (reactive) unit templates (u_{qa}, u_{qb}, u_{qc}), can be written as,

$$\left\{\begin{array}{c} u_{qa} = -u_{pb}/\sqrt{3} + u_{pc}/\sqrt{3} \\ u_{qb} = \sqrt{3}u_{pa}/2 + (u_{pb} - u_{pc})/2\sqrt{3} \\ u_{qc} = -\sqrt{3}u_{pa}/2 + (u_{pb} - u_{pc})/2\sqrt{3} \end{array}\right\} \tag{3}$$

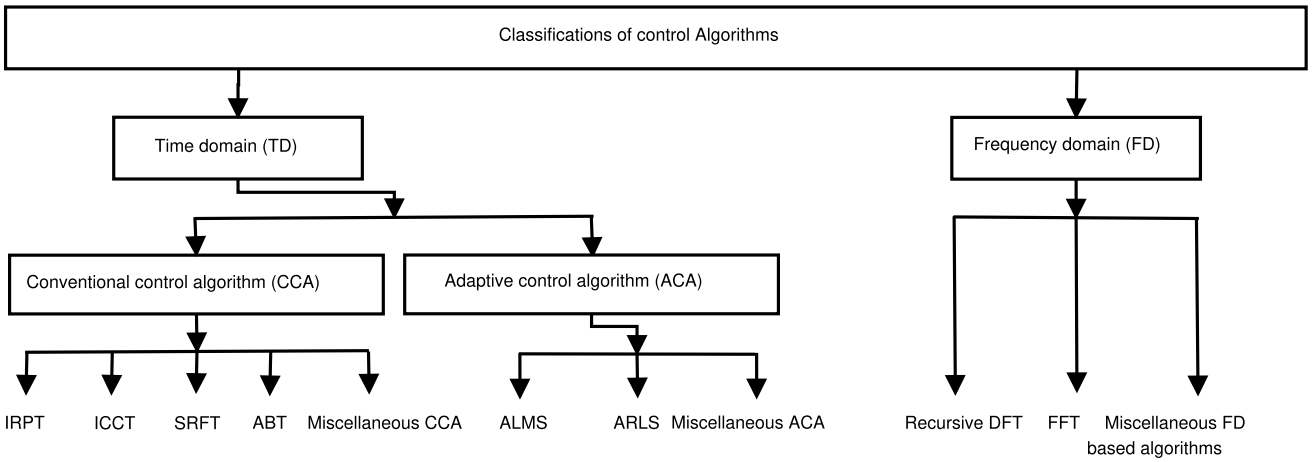

FIGURE 4. General classification of control algorithms.

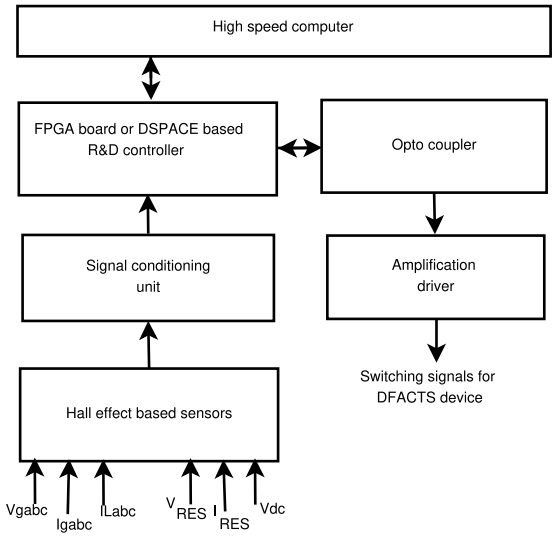

FIGURE 5. Basic building block of general hardware framework of a control algorithm for DFACTS devices.

- **Estimation of Loss components**: PI voltage regulator is used to generate active and reactive loss components. Reactive loss component ($i_{qr}(n)$) is utilized to maintain terminal voltage at PCC, this is derived from PI voltage regulator.

$$i_{qr}(n) = i_{qr}(n-1) + k_{pq}(v_{te}(n) - v_{te}(n-1)) + k_{iq}v_{te}(n) \quad (4)$$

where, $i_{qr}(n-1)$ and $v_{te}(n-1)$ are preceding value of reactive loss component and voltage error. The current value of this voltage error ($v_{te}(n)$) is calculated as,

$$v_{te}(n) = v_{tn}(n) - v_t(n) \quad (5)$$

where, v_{tn} represents the peak amplitude of phase voltage and taken as reference value of terminal voltage (v_t). PI voltage regulator maintains the dc bus voltage by calculating active loss component ($i_{dr}(n)$).

$$i_{dr}(n) = i_{dr}(n-1) + k_{pd}(v_{de}(n) - v_{de}(n-1)) + k_{id}v_{de}(n) \quad (6)$$

where, $i_{dr}(n-1)$ and $v_{de}(n-1)$ are the preceding value of active loss component and dc voltage error. However, the current value of this dc voltage error is,

$$v_{de}(n) = v^*_{dc}(n) - v_{dc}(n) \quad (7)$$

where, v^*_{dc}; reference DC bus voltage calculated as ($v^*_{dc} = 2\sqrt{2}v_{LL}/\sqrt{3}m$). v_{LL} represents voltage (line to line) at PCC, m is modulation index. v_{dc}; actual DC link voltage.

- **Extraction of fundamental component of load currents**: The computation of active and reactive component of load current depends on 3-phase to 2-phase and 2-phase to 3-phase conversion methodology used in the control algorithms.
- **Generation of three-phase reference signals**: The extracted in-phase and quadrature load currents obtained using PLL circuit are corrected with the help of voltage unit templates to derive active and reactive components of grid current signals. These components are combined to generate reference grid signals using 2-phase to 3-phase conversion. The details of the reference current generation signals may vary with the type of algorithm.
- **Generation of gating signals**: The generated 3-phase reference signals (i^*_{sabc}) along with actual grid signals (i_{sabc}) are fed to pulse width modulation based controller to generate gating signals for DFACTS devices.
Note: The gating signals for the fourth leg switches of DFACTS device in 3P4W utility grid are calculated from the current error signal by comparing sensed neutral signal (i_{sn}) and reference neutral signal (i^*_{sn}). These signals are calculated as,

$$\left\{\begin{array}{c} i^*_{sn} = 0 \\ i_{sn} = -(i_{sa} + i_{sb} + i_{sc}) \end{array}\right\} \quad (8)$$

The implementation of the generalized approach of conventional control has been implemented in various conventional control algorithms as detailed in following subsections.

2) INSTANTANEOUS REACTIVE POWER (IRPT) CONTROL THEORY

The concept of IRPT was first proposed by H. Akagi and has been used for generation of the reference signal for DFACTS devices to mitigate PQ issues. The basic working methodology of this theory includes the transformation (3-phase to 2-phase) and reverse transformation (2-phase to 3-phase) of voltage and current quantities for the estimation of reference current signal. The computations involved in the IRPT theory to estimate instantaneous active (p) and reactive (q) components of current signals have been presented in [94]. The basic building block of IRPT is depicted in Fig 6. The 3-phase voltage (V_{sabc}) and load currents (i_{Labc}) are converted in to α-β-0 components using Clark transformation and zero sequence component of active power is suppressed. The loss component (*loss*) is estimated using the PI regulator. This loss component is combined to average (dc) part of the active instantaneous power ($\bar{p}$) for estimating ($\bar{p}_{loss}$). This component and average (dc) part of the instantaneous reactive power ($\bar{q}$) are combined to calculate i_α and i_β current signals. These signals in-turn are utilized to generate reference current signals with the help of reverse Clark's transformation. These reference signals and actual grid signals are fed to the HCC to generate gating signals for DFACTS device.

$$\begin{bmatrix} i^*_{sa} \\ i^*_{sb} \\ i^*_{sc} \end{bmatrix} = \sqrt{2/3} \begin{bmatrix} 1/\sqrt{2} & 1 & 0 \\ 1/\sqrt{2} & -1/2 & \sqrt{3}/2 \\ 1/\sqrt{2} & -1/2 & -\sqrt{3}/2 \end{bmatrix} \times \begin{bmatrix} i^*_{s0} \\ i^*_{s\alpha} \\ i^*_{s\beta} \end{bmatrix} \quad (9)$$

where, i^*_{s0}: zero sequence component and it is zero in 3P3W utility grid, $\bar{P}$: average (dc) part of the instantaneous power, $i^*_{s\alpha}$ and $i^*_{s\beta}$: reference grid signals, $\Delta = v^2_\alpha + v^2_\beta$, α and β: orthogonal coordinates,

$$\begin{bmatrix} i^*_{s\alpha} \\ i^*_{s\beta} \end{bmatrix} = 1/\Delta \begin{bmatrix} v_\alpha & -v_\beta \\ v_\beta & v_\alpha \end{bmatrix} \times \begin{bmatrix} \bar{P} \\ 0 \end{bmatrix} \quad (10)$$

3) INDIRECT CURRENT CONTROL THEORY

The basic building block of ICCT is illustrated in Fig 7. In ICCT control theory, 3-phase grid voltages are utilized for the computation of 3-phase reference currents. These reference currents consist of in-phase component (active component) and out-phase component (quadrature component) as presented in [95], [96]. The active reference current (I^*_{smd}) component is kept constant. This constant depends on the unit vector templates (u_{abc}) and active power required by the load. This unit template is multiplied by reference current (I^*_{smd}) to obtain reference active component of current ($i^*_{sabc_d}$). The PI controller provides quadrature component of the reference current signal (I^*_{smq}) by comparing terminal voltage (v_t) with its reference voltage (v^*_t). This current signal is multiplied

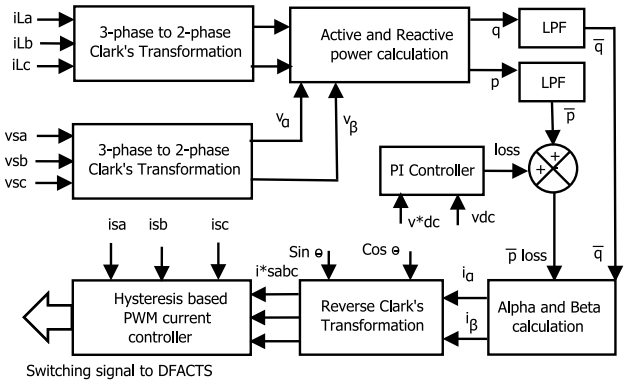

FIGURE 6. Basic building block of IRP theory.

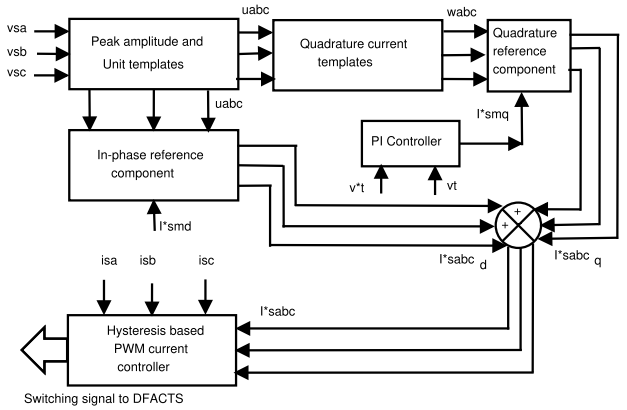

FIGURE 7. Basic building block of ICCT.

by quadrature template (w_{abc}) to obtain reference quadrature component of current ($i^*_{sabc_q}$). Both the ($i^*_{sabc_d}$) and ($i^*_{sabc_q}$) component of currents are combined to generate reference current signals (i^*_{sabc}). The estimated reference current signals are compared with actual 3-phase grid signals (i_{sabc}) to generate gating signals for DFACTS device.

$$i^*_{sabc_d} = i^*_{smd} \times u_{abc} \quad (11)$$

$$i^*_{sabc_q} = i^*_{smq} \times w_{abc} \quad (12)$$

4) SYNCHRONOUS REFERENCE FRAME CONTROL THEORY

SRFT control theory is based on the sensed load current and grid voltage signals [97]–[99]. The basic building block of SRFT is illustrated in Fig 8. The 3-phase current signals have been converted into α-β-0 axes using Clark transformation. This frame is further transformed in to d-q-0 frame to obtain direct-axis (i_d) and quadrature-axis (i_q) current components. These d-q components are filtered with the help of LPF to obtain (i_{ddc}) and (i_{qdc}) components. The reference direct axis current (i^*_{ddc}) is generated by adding filtered direct axis component (i_{ddc}) with direct axis loss component (i_{dloss}). This (i_{dloss}) loss component is perceived by comparing dc link voltage (v_{dc}) with its reference voltage (v^*_{dc}) using DC proportional integral controller. The quadrature axis (i^*_{qdc})

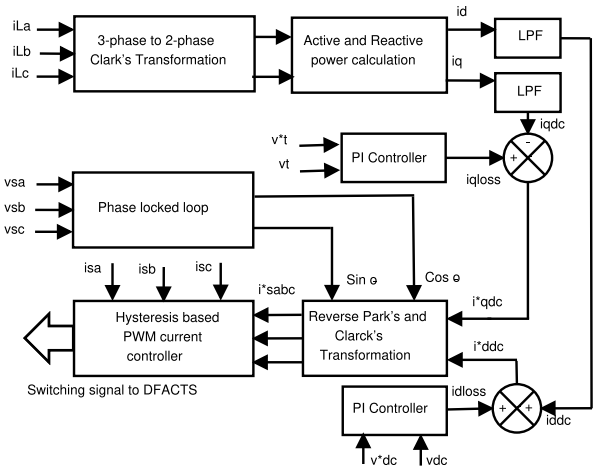

FIGURE 8. Basic building block of SRF theory.

component is computed by subtracting filtered quadrature (i_{qdc}) component and quadrature axis loss component (i_{qloss}). This i_{qloss} component is obtained by comparing terminal voltage (v_t) with its reference voltage (v_t^*) using ac PI controller. Finally, the reference signals in a–b–c frame are obtained by reverse Park's and Clark's transformation using PLL. The estimated reference signals are compared with actual 3-phase grid signals (i_{sabc}) to generate gating signals for DFACTS device.

$$\begin{bmatrix} i_{sa}^* \\ i_{sb}^* \\ i_{sc}^* \end{bmatrix} = \sqrt{2/3} \begin{bmatrix} 0 & 1 & 1 \\ 0 & -1/2 & \sqrt{3}/2 \\ 0 & -1/2 & -\sqrt{3}/2 \end{bmatrix} \times \begin{bmatrix} i_{s0}^* \\ i_{s\alpha}^* \\ i_{s\beta}^* \end{bmatrix} \quad (13)$$

where,

$$\begin{bmatrix} i_{s0}^* \\ i_{s\alpha}^* \\ i_{s\beta}^* \end{bmatrix} = \begin{bmatrix} 1 & 0 & 0 \\ 0 & cos\theta & -sin\theta \\ 0 & sin\theta & cos\theta \end{bmatrix} \times \begin{bmatrix} 0 \\ i_d^* \\ i_q^* \end{bmatrix} \quad (14)$$

5) ADMITTANCE BASED CONTROL THEORY

In this theory the active (p) and reactive (q) components are estimated using voltage and current signals of the system [100]. The basic building block of ABT is illustrated in Fig 9. The active unit template (u_{abc}) and quadrature unit template (w_{abc}) are estimated using 3-phase grid voltages. These unit templates and load currents are combined to generate instantaneous active and reactive current components. This p-q components filtered by low pass filter with appropriate frequency to obtain active (P_{dc}) and reactive (Q_{dc}) components. The reference active power (P_r) is divided by the constant value computed using terminal voltage (v_t) to obtain reference conductance (G_{pt}). The PI voltage regulator produce the desired amount of reactive power (Q_{cv}) for voltage control to compensate reactive power fluctuations at PCC. The output of PI voltage regulator (Q_{cv}) is deducted by the 3-phase load reactive power (Q_{dc}) of grid current to compute (Q_r) component of dc current. Further, this component is divided by the constant value computed using terminal voltage (v_t) to

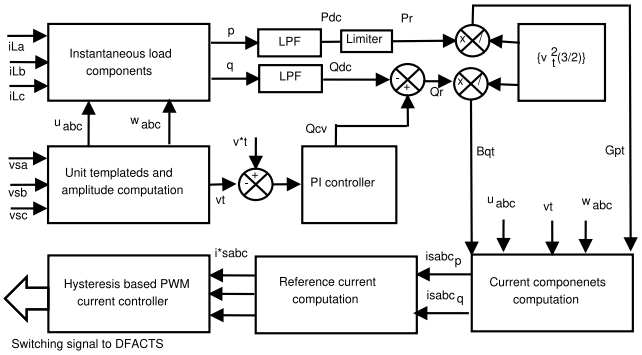

FIGURE 9. Basic building block of Admittance based theory.

obtain reference susceptance (B_{qt}). These computed signals help to obtain fundamental active (i_{sabc_p}) and quadrature (i_{sabc_q}) current components. Both signals are combined to obtain reference grid current signals. The estimated reference signals are compared with actual 3-phase grid signals (i_{sabc}) to generate gating signals for DFACTS device.

$$i_{sabc_p} = G_{pt} \times v_t \times u_{abc} \quad (15)$$

$$i_{sabc_q} = B_{qt} \times v_t \times w_{abc} \quad (16)$$

where,

$$G_{pt} = P_r/(v_t^2(3/2)) \quad (17)$$

$$B_{qt} = Q_r/(v_t^2(3/2)) \quad (18)$$

6) MISCELLANEOUS CONVENTIONAL CONTROL ALGORITHM

Apart from the algorithms mentioned in the above section, the other conventional control algorithms have played an important role in PQ mitigation with DFACTS devices. These includes, power balance control [101], instantaneous symmetrical components control [102], sliding mode control (SMC) [103], average unit power factor control [104], voltage template and PI controller [105], PLL based control [106] and their modified methods. However, the experimental framework for conventional control algorithms has not been extensively used with RE penetration in the utility grid.

It has been reported that the compatibility and performance of conventional control algorithms with RE penetration are not providing good results as expected. Hence, the performance of these algorithms is low compared to adaptive control algorithms due to limitations as described in Table 5. The conventional control algorithms use complex circuitry like PLL, 3-phase to 2-phase conversion blocks, 2-phase to 3-phase conversion blocks. Therefore computational complexity associated with these algorithms is high and dynamic response is found be slow. Hence, the performance of conventional control algorithms is poor in mitigating the harmonics. However, when these algorithms are burn in the hardware-based R&D controllers like DSP, the oscillations are found to be high in computational speed and DC link voltage.

TABLE 5. Limitations of conventional control algorithms.

S.No.	Limitations
1.	Complex circuitry like PLL is required.
2.	High computation the dynamic response is slow and more complex.
3.	DC link voltage and DSP speed oscillations are high.
4.	Accuracy is medium due to poor stability.
5.	THD calculation is not accurate due to low dynamic response.

B. ADAPTIVE CONTROL ALGORITHMS

To enhance the power quality of grid integrated RE sources with DFACTS devices, researchers have started switching to adaptive signal processing based algorithms. These control algorithms work on continuous updating of weight component of current and voltage signals based on the initial values, old estimation and system changes for the estimation of reference gate signals. The simplest algorithm presented in literature is based on the Least Mean Square (LMS). This algorithm was proposed by Widrow *et al.* [107]. The notability of the LMS algorithm is easy for implementation. The implementation of neural network-based LMS controlled VSC for PQ mitigation has been presented in [108], [109]. This algorithm is also used in mobile communication [110], [111]. However, this LMS algorithm becomes unstable where the signal to noise ratio (SNR) is low. LMF, which is fourth-order error correction algorithm exhibits stability even with low SNR values [112] as static error and mean square error associated with LMF control is lower compared to LMS algorithm [113]. The LMS/F algorithms found to be classical methods for adaptive system identification (ASI) [114]. The details of the implementation of the recursive least-squares algorithm are presented in [115]. This adaptive algorithm provides better convergence and highly correlated input signals compared to the LMS algorithm. The price to pay for this is an increase in computational complexity. Variable forgetting factor recursive least-squares (VFFRLS) algorithm has been developed in [116], [117]. This algorithm has reduced computational complexity and ability to adopt various changes in the system to obtain desired signals for solving complexity and stability issues [118], [119].

1) DESIGN OF ADAPTIVE CONTROL ALGORITHM

The various design steps involved in adaptive control algorithms are detailed below. Standard notation and nomenclature are used based on the research articles cited in this review.

- **Estimation of active and reactive unit templates**: 3-phase line voltages (v_{sab}, v_{sbc}) are utilized to obtain phase voltages using the following relation,

$$\left.\begin{array}{l} v_{sa} = (2v_{sab} + v_{sbc})/3 \\ v_{sb} = (-v_{gab} + v_{sbc})/3 \\ v_{sc} = (-v_{sab} - 2v_{sbc})/3 \end{array}\right\} \tag{19}$$

Peak amplitude of terminal voltage (v_t) is given as,

$$v_t = \sqrt{2/3(v_{sa}^2 + v_{sb}^2 + v_{sc}^2)} \tag{20}$$

Three-phase in-phase (active) unit vector templates (u_{pa}, u_{pb}, u_{pc}) are given as,

$$u_{pa} = v_{sa}/v_t, \quad u_{pb} = v_{sb}/v_t, \; u_{pc} = v_{sc}/v_t \tag{21}$$

Three-phase quadrature (reactive) unit templates (u_{qa}, u_{qb}, u_{qc}) are given as,

$$\left.\begin{array}{c} u_{qa} = -u_{pb}/\sqrt{3} + u_{pc}/\sqrt{3} \\ u_{qb} = \sqrt{3}u_{pa}/2 + (u_{pb} - u_{pc})/2\sqrt{3} \\ u_{qc} = -\sqrt{3}u_{pa}/2 + (u_{pb} - u_{pc})/2\sqrt{3} \end{array}\right\} \tag{22}$$

- **Estimation of loss components**: PI voltage regulator is used to generate the active and reactive loss components. Reactive loss component (W_{cq}) is utilized to maintain terminal voltage at PCC.

$$W_{cq}(n+1) = W_{cq}(n) + k_{pq}(v_{te}(n+1) - v_{te}(n)) + k_{iq}v_{te}(n+1) \tag{23}$$

where, $W_{cq}(n+1)$ and $v_{te}(n+1)$ are updated reactive loss component and voltage error. The current value of this voltage error is computed as,

$$v_{te}(n) = v_{tn}(n) - v_t(n) \tag{24}$$

This regulator maintains dc link voltage by generating active loss component (W_{cp}).

$$W_{cp}(n+1) = W_{cp}(n) + k_{pd}(v_{de}(n+1) - v_{de}(n)) + k_{id}v_{de}(n+1) \tag{25}$$

where, $W_{cp}(n+1)$ and $v_{de}(n+1)$ are the updated active loss component and dc voltage error. The current value of this dc voltage error is,

$$v_{de}(n) = v_{dc}^*(n) - v_{dc}(n) \tag{26}$$

where, v_{dc}^*; reference DC bus voltage calculated as ($v_{dc}^* = 2\sqrt{2}v_{LL}/\sqrt{3}m$). v_{LL} represents voltage (line to line) at PCC, m is modulation index. v_{dc}; actual DC link voltage. Note: In case of RE penetration v_{dc}^* perceived from the maximum power point tracking (MPPT) based algorithm. However, output of these algorithms depends on the type of RE sources.

- **Estimation of feed forward term**: The feed forward term (W_{RES}) is computed based on current output power (P_{RES}) of RES given by,

$$W_{RES}(n) = 2P_{RES}(n)/3v_t \tag{27}$$

- **Extraction of fundamental weight component of load current**: The extraction of active and reactive weight component of load current depends on weight updation methodology used in the control algorithms. Let, the basic load current equation of AC distribution network is given as,

$$i_L(t) = Isin(wt + \phi) + \Sigma I_n sin(nwt + \phi_n) \tag{28}$$

It can also be represented as,

$$i_L(t) = i(t) + i_h(t) = i_p(t) + i_q(t) + i_h(t) \tag{29}$$

where, $i(t)$ is the fundamental current component which is made up of active current $i_p(t)$ and reactive current $i_q(t)$ whereas $i_h(t)$ is the harmonic current components. The initial estimation of the active, reactive part of load current and harmonic parts of load current for a single-phase is given as,

$$i_p(t) = W_p \times u_p, i_q(t) = W_q \times u_q \tag{30}$$

$$i_h(t) = i_L(t) - i_p(t) - i_q(t) \tag{31}$$

The weights (W_p) and (W_q) are not constant values, and continuously update according to the changes associated with system. Active unit voltage template (u_p) and reactive unit voltage template (u_q) are calculated using grid voltages.

- **Estimation of total active and reactive weight components**: The total active weight component (W_{sp}) is calculated by adding dc loss component (W_{cp}) to average active weight component (W_{Lpa}) and deducting the feed-forward RES weight component (W_{RES}),

$$W_{sp} = W_{Lpa} + W_{cp} - W_{RES} \tag{32}$$

where,

$$W_{Lpa} = (W_{pa} + W_{pb} + W_{pc})/3 \tag{33}$$

Similarly, the total reactive weight component (W_{sq}) is calculated by subtracting the average reactive weight component (W_{Lqa}) to the ac loss component (W_{cq}),

$$W_{sq} = W_{cq} - W_{Lqa} \tag{34}$$

where,

$$W_{Lqa} = (W_{qa} + W_{qb} + W_{qc})/3 \tag{35}$$

- **Generation of three-phase reference signals**: The active reference signal (i^*_{pabc}) is estimated using total active weight component (W_{sp}) and 3-phase active unit templates.

$$i^*_{pabc} = W_{sp} \times u_{pabc} \tag{36}$$

Similarly, the reactive reference signal (i^*_{qabc}) is estimated using reactive weight component (W_{sq}) and 3-phase active unit templates.

$$i^*_{qabc} = W_{sq} \times u_{qabc} \tag{37}$$

Thus, 3-phase reference grid current signals are generated by combining active reference signal (i^*_{pabc}) and reactive reference signal (i^*_{qabc}),

$$i^*_{sabc} = i^*_{pabc} + i^*_{qabc} \tag{38}$$

Note: The details of the reference current generation may vary with the type of algorithm.

- **Generation of gating signals**: The generated 3-phase reference signals (i^*_{sabc}) along with actual grid signals (i_{sabc}) are fed to pulse width modulation based controller to generate gating signals for DFACTS devices.

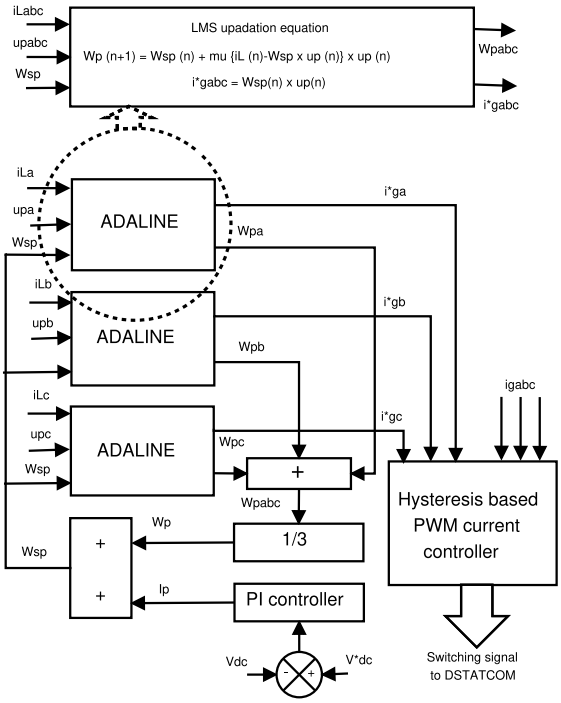

FIGURE 10. Basic building block of ADALINE Algorithm.

Note: The gating signals for the fourth leg switches of DFACTS device in 3P4W utility grid are calculated from the current error signal by comparing sensed neutral signal (i_{sn}) and reference neutral current signal (i^*_{sn}). These current signals are calculated as,

$$\left\{\begin{matrix} i^*_{sn} = 0 \\ i_{sn} = -(i_{sa} + i_{sb} + i_{sc}) \end{matrix}\right\} \tag{39}$$

The implementation of the generalized approach of adaptive control has been implemented in various adaptive control algorithms with RE penetration as detailed in following sub-sections.

2) ADAPTIVE LINEAR ELEMENT (ADALINE) CONTROL THEORY

The basic building block of ADALINE control theory is illustrated in Fig 10. The extraction of in-phase component of the load current signals is carried out using NN based LMS algorithm known as ADALINE theory. This control algorithm tracks and estimates the in-phase unit templates (u_{pabc}) using 3-phase grid voltages, so as to maintain minimum error. The unit templates and initial weight components are corrected with the help of 3-phase load currents to estimate current error (e_{pabc}). These initial weights are initialized randomly. The weights are continuously updated until least mean square error is obtained [31], [120], [121] The weights are updated using following equation,

$$W_{pabc}(n+1) = W_{pabc}(n) + \mu(e_{pabc}) \times u_{pabc}(n) \tag{40}$$

$$e_{pabc}(n) = i_{Labc}(n) - W_{pabc}(n) \times u_{pabc}(n) \tag{41}$$

The new weight component is updated by adding the product of the current error component and unit vector component along with adaptive constant (μ). This adaptive constant is kept between the range [0-1] to obtain desired results [122], [123]. The updated weights are averaged to eliminate the effect of unbalancing in the current components. The PI controller provides in-phase component (I_p) by comparing dc-link voltage (v_{dc}) with its reference voltage (v^*_{dc}). This in-phase component (I_p) and averaged weight (W_p) components are added to obtain updated weight components (W_{sp}). The 3-phase reference signals are generated using updated weight W_{sp} component and in-phase unit templates [30]. The estimated reference signals are compared with actual 3-phase grid signals to generate gating signals for DFACTS device.

3) ADAPTIVE LEAST MEAN SQUARE (ALMS) CONTROL ALGORITHM

The basic building block of adaptive least mean square (ALMS) control algorithm is illustrated in Fig 11. This algorithm computes fundamental active (p) and reactive (q) weight components of load currents considering the grid voltages and RE source generation [113], [124], [125]. In this control algorithm, the new reactive weight component is updated by adding the product of reactive current error component ($e_{qabc}(n)$) and reactive voltage unit vector component along with adaptive constant (τ_q). These updated reactive weights (W_{qabc}) are averaged to eliminate the effect of unbalancing in the reactive current components. This averaged weight components are passed through LPF with appropriate frequency to perceive average fundamental reactive weight component (W_{Lqa}). This (W_{Lqa}) component is deducted from reactive loss component (W_{cq}), which is the output of a PI controller processing voltage error to obtain reactive weight component (W_{sq}). This reactive weight component (W_{sq}) and reactive unit templates (u_{qabc}) are combined to generate 3-phase reactive reference currents (i^*_{qabc}).

$$W_{qabc}(n+1) = W_{qabc}(n) + \tau_q \times u_{qabc}(n) \times e_{qabc}(n) \quad (42)$$

$$e_{qabc}(n) = i_{Labc}(n) - u_{qabc}(n) \times W_{qabc}(n) \quad (43)$$

$$i^*_{qabc} = W_{sq} \times u_{qabc} \quad (44)$$

Similarly, the new active weight component is updated by adding the product of active current error component ($e_{pabc}(n)$) and active voltage unit vector component along with adaptive constant (τ_p). These updated active weights (W_{pabc}) are averaged to eliminate the effect of unbalancing in the active current components. These averaged weight components passed through the LPF to suppress ripples for obtaining average fundamental active weight component (W_{Lpa}). The total active weight component (W_{sp}) of grid currents are evaluated by combining the dc loss component (W_{cp}) to average fundamental active weight component (W_{Lpa}) and the feed-forward RE sources (W_{RES}) weights. The active loss component (W_{cp}) is obtained using PI controller by comparing DC link voltage with its reference voltage (v^*_{dc}). This reference value of DC link voltage is computed

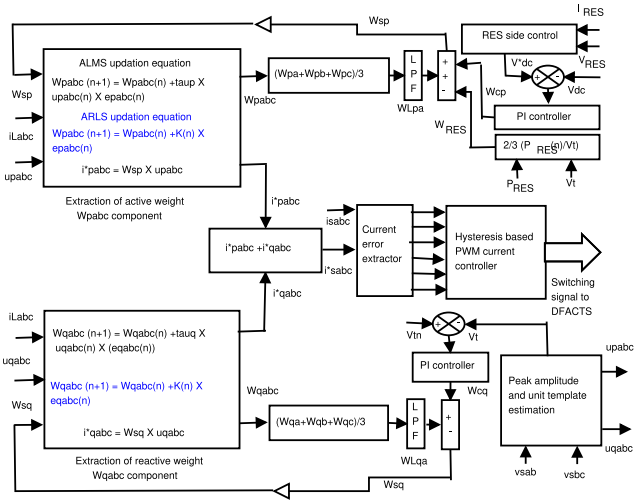

FIGURE 11. Basic building block of ALMS and ARLS algorithms.

using RES current and voltages. The feed-forward term of RE sources (W_{RES}) is obtained by combining the output power of RE sources (P_{RES}) and terminal voltage (v_t). This computed active weight component (W_{sp}) and active voltage unit templates (u_{pabc}) are combined to generate 3-phase active reference currents (i^*_{pabc}).

$$W_{pabc}(n+1) = W_{pabc}(n) + \tau_p \times u_{pabc}(n) \times e_{pabc}(n) \quad (45)$$

$$e_{pabc}(n) = i_{Labc}(n) - u_{pabc}(n) \times W_{pabc}(n) \quad (46)$$

$$i^*_{pabc} = W_{sp} \times u_{pabc} \quad (47)$$

Both 3-phase reactive reference current (i^*_{qabc}) and active reference current (i^*_{pabc}) signals are added to obtain reference grid current signals. The estimated reference current signals are compared with actual 3-phase grid current signals to generate gating signals for DFACTS device [67], [126].

$$i^*_{sabc} = i^*_{pabc} + i^*_{qabc} \quad (48)$$

4) ADAPTIVE RECURSIVE LEAST SQUARE CONTROL ALGORITHM

The basic building block of adaptive recursive least square (ARLS) control algorithm is illustrated in Fig 11 with blue color coding. This algorithm computes fundamental active (p) and reactive (q) weight components of load currents considering the grid voltages and RE source generation [116]. The cost function j(n) is expressed as,

$$Costfunctionj(n) = \sum_{k=1}^{(n)} \eta_n(n) e^2(n) \quad (49)$$

where, n is represented as variable length of observed data, $\eta_n(n)$ is weighting factor and e(n) is error component. Likewise, Kalman gain is estimated using following equation,

$$k(n) = [P(n-1)u(n)]/[\lambda + u^T(n)P(n-1)u(n)] \quad (50)$$

$$P(n) = 1/\lambda[P(n-1) - k(n)u^T(n)P(n-1)] \quad (51)$$

where, Kalman gain k(n), inverse of input signal correlation matrix P(n) and input unit template vector u(n). The learning of the algorithm is based on the forgetting factor (λ). The tracking capability and convergence rate of ARLS depends on forgetting factor (FF) [127]. This FF lies between 0 to 1 [128], [129]. Low value of FF provides better tracking capability and slow convergence rate and high value of FF (near to 1) provides low tracking capability and fast convergence rate.

In this control algorithm, the new reactive weight component is updated by adding the product of reactive current error component ($e_{qabc}(n)$) and reactive Kalman gain ($K_q(n)$) component. These updated weights (W_{qabc}) are averaged to eliminate the effect of unbalancing in the reactive current components. This averaged weight components passed through low pass filter to perceived average fundamental reactive weight component (W_{Lqa}). This (W_{Lqa}) component is deducted from reactive loss component (W_{cq}), which is the output of an PI controller processing voltage error to obtain reactive weight component (W_{sq}). This (W_{sq}) component and reactive unit templates (u_{qabc}) are combined to generate 3-phase reactive reference currents (i^*_{qabc}).

$$W_{qabc}(n+1) = W_{qabc}(n) + k_q(n) \times e_{qabc}(n) \quad (52)$$

$$e_{qabc}(n) = i_{Labc}(n) - W_{qabc} \times u_{qabc}(n) \quad (53)$$

$$i^*_{qabc} = W_{sq} \times u_{qabc} \quad (54)$$

Similarly, the new active weight component is updated by adding the product of active current error component ($e_{pabc}(n)$) and active Kalman gain ($K_p(n)$) component. These updated weights (W_{pabc}) are averaged to eliminate the effect of unbalancing in the active current components. This averaged weight components passed through the LPF to suppress ripples for obtaining average fundamental active weight component (W_{Lpa}). The total active weight component (W_{sp}) of grid currents combining from the dc loss component (W_{cp}) to average fundamental active weight component (W_{Lpa}) and the feed forward RE source (W_{RES}) weights. The active loss component (W_{cp}) is obtained using PI controller by comparing DC link voltage (v_{dc}) with its reference voltage (v^*_{dc}). This (v^*_{dc}) voltage is computed using RES current and voltages. The feed forward term of RE sources (W_{RES}) is obtained by combining output power of RE sources (P_{RES}) and terminal voltage (v_t). This computed active weight component (W_{sp}) and active voltage unit templates (u_{pabc}) are combined to generate 3-phase active reference currents (i^*_{pabc}).

$$W_{pabc}(n+1) = W_{pabc}(n) + k_p(n) \times e_{pabc}(n) \quad (55)$$

$$e_{pabc}(n) = i_{Labc}(n) - W_{pabc} \times u_{pabc}(n) \quad (56)$$

$$i^*_{pabc} = W_{sp} \times u_{pabc} \quad (57)$$

Both 3-phase reactive reference current (i^*_{qabc}) and active reference current (i^*_{pabc}) signals are added to obtain reference grid current signals. The estimated reference signals are compared with actual 3-phase grid signals to generate gating signals for DFACTS device.

$$i^*_{sabc} = i^*_{pabc} + i^*_{qabc} \quad (58)$$

TABLE 11. Feasibility and economic consideration of grid tied RES.

Factors	Illustration
Grid integration	There is no requirement of large-capacity batteries in grid tied RES with DFACTS systems. For similar loads grid-tied system use smaller RES compare to stand-alone systems.
Distance to utility network	Grid-tied RES with DFACTS systems should be integrated into utility grid as nearest as possible to avoid unnecessary operations. Stand-alone systems have a big issue, as it is located far from electrical utility networks, which is uneconomical. Distance is increasing losses are also, increases with the length of the line.
Balance of system components	International safety standards and regulations may require for new balance of 3P3W and 3P4W utility system. Initial costs for installation are depending on the balance of system components.
Installation cost	Per watt basis, large scale grid-tied RES with DFACTS systems tend to be economical. Grid-tied RES with DFACTS systems endows lower initial cost with the energy costs for heavy loads.
Maintenance	There are no moving parts in small scale grid-tied RES with DFACTS systems, so notable maintenance costs is zero percent.
Energy use and cost	Energy use is a crucial factor in deciding system size. Reducing energy consumption due to small RES with DFACTS systems greatly reduces the initial capital cost investment.

5) MISCELLANEOUS ADAPTIVE CONTROL ALGORITHMS

Apart from the algorithms mentioned in above section, the other adaptive signal processing based control algorithms have played an important role in PQ mitigation in association with DFACTS devices in utility grids integrated with RE sources. These includes, Filtered-X LMS control algorithm [159], adaptive notch filter based multipurpose technique [131], [150], Back-Propagation control control [147], adaptive filter [148], modified synchronous detection [149], kernel incremental meta-learning algorithm [151], adaptive linear optimal filter [160], empirical mode decomposition [153], adaptive learning-based anti-Hebbian [146], noise cancellation [161], adaptive notch filter (ANF) [157], automatic synchronization control control [162], ANFIS based control [163], proportional resonant integral (PRI) controller [164], optimized reactive power compensation algorithm (RPCA) [165], adaptive observer-based harmonic cancellation technique [130], non-linear adaptive controller [166], anti-windup [167], damped second order generalized integrator (DSOGI) [168], [169], decoupled adaptive noise detection (DAND) [170], admittance LMS neural network [126], LMF algorithm [171], combined LMS-LMF [172], momentum least mean square (MLMS) [173], improved linear sinusoidal tracer (ILST) [174], [175] and modified RLS [128]. These algorithms for DFACTS devices have been established successfully and validated by hardware framework.

State of the art, clearly establishes that adaptive signal processing based control algorithms provide ease for estimation of the active component and reactive component along with the less computational complexity. These algorithms exhibit robustness and faster response. The performance of various conventional and adaptive control algorithms has been analyzed by selecting various parameters of these algorithms used in recent research as listed in Table 6. However, Table 7 shows the experimental data-based performance analysis of these algorithms. In Table 7, parameters have been selected based on the laboratory-based experimental data from the respective references. It has been perceived from the tabled data that, the implementation of adaptive control algorithms

TABLE 6. Performance analysis of various control algorithms for PQ improvement.

Parameters	Conventional Control Algorithms				Adaptive Control Algorithms		
	ICCT	IRPT	SRFT	Admittance	Adaline	ALMS	ARLS
Nature of Controlling	Non-adaptive	Non-adaptive	Non-adaptive	Non-adaptive	Adaptive	Adaptive	Adaptive
Reactive power compensation	Average	Good	Good	Very Good	Very Good	Excellent	Excellent
Harmonic mitigation	Average	Average	Good	Good	Very Good	Excellent	Excellent
Power factor correction	Average	Good	Very Good	Good	Excellent	Excellent	Excellent
Load balancing	Good	Good	Good	Good	Good	Very Good	Good
Grid neutral current elimination	Good	Good	Very Good	Good	Good	Very Good	Very Good
Regulation of DC link voltage	Average	Average	Good	Good	Good	Excellent	Good
Robustness	Poor	Poor	Good	Average	Very Good	Excellent	Excellent
Flexibility	Poor	Poor	Good	Average	Very Good	Excellent	Good
Convergence	-	-	-	-	Good	Excellent	Excellent
Performance with RES	Poor	Poor	Good	Good	Very Good	Excellent	Excellent
Computational complexity	Poor	Poor	Average	Poor	Average	Average	Average

TABLE 7. Performance analysis of various control algorithms based on experimental datas.

Parameters	SRFT	LMS	LMF	VSLMS	ANFIS LMS	Adaptive NN	Adaptive Observer	RLS	VFFRLS
	[114]			[69]		[127]	[131]	[119]	
Type	Time domain PLL based	Adaptive filter	Adaptive filter	Stochastic gradient approach	-	-	Adaptive feed-forward cancellation	Least square estimation	Least square estimation
Input signal	-	Stochastic	Stochastic	Stochastic	Stochastic	-	-	Deterministic	Deterministic
Computation complexity	High	Low	Low	High	Low	Low	-	Less	Moderate
Order of optimization	-	2^{nd} order	4^{th} order	-	-	-	-	-	-
Static error	-	More	Less	Medium	Less	-	Better	Less	Less
Dynamic response	Slow	Medium	Fast	Fast	Fast	Fast	Fast	Medium	Fast
MSE	-	19.79	17.02	-	-	-	-	-	-
Computations	More	Less	Less	Less	Less	Less	Medium	Less	Less
DSP speed	High	Low	Low	Low	Low	High	Medium	Medium	Low
Convergence rate	-	Oscillate at mean value	Oscillate at mean value	Oscillate at mean value	0.1sec	-	-	Oscillate at mean value	0.15 sec
Sampling time (Ts)	-	50 μ sec	50 μ sec	60 μ sec	60 μ sec	30 μ sec	-	50 μ sec	60 μ sec
Step size (μ)	-	Fix	-	Variable	Variable	-	-	Fix	Variable
Accuracy	Poor	Medium	High	High	High	High	Medium	Medium	High
Stability	-	Good	Better	Good	Better	Good	Good	Good	Better
THD (%)	-	i_S = 4.29	i_S = 1.12	i_S = 3.62	i_S =2.57	i_S =2.92	i_S = 3.00	i_S = 3.68	i_S = 2.44
	-	i_L = 26.66	i_L = 27.24	i_L = 26.66	i_L = 26.7	i_L = 25.6	i_L = 25.9	i_L = 26.95	i_L =26.95

TABLE 8. Performance analysis of 3P3W and 3P4W system in isolated mode.

Achievements	System	RSGA	Regulator	Comparator	DFACTS devices	Ref.
During load perturbation Amplitude adaptive notch filter algorithm has been provided transient free operation of the grid to maintain unity power factor (UPF). Also, the complexity of the control circuit has been reduced.	3P3W, programmable AC, 415V, 50 Hz	ANF based dq scheme	-	SPWM	DSTATCOM	[132]
Voltage control, harmonic mitigation has been achieved under N-L loads. Also, the integrated electronic load controller scheme with NN (NNIELC) found to be less complicated and sensitive in load balancing.	3P4W, 3.7 kW, 230V 50-Hz, 4-Pole,Asy. m/c	NNIELC	PI	PWM	VSC	[133]
Current harmonics has been mitigated with maintaining power factor unity. Also, balancing of loads and voltage regulation has been achieved under linear and N-L load.	3P3W, IG-3.7kW, IM -3.7kW, 415V,50Hz	Composite observer	PI	PWM	DSTATCOM	[134]
Harmonics have been eliminated using Filtered-X-LMS (FXLMS) algorithm in-presence of diesel engine (DE).	3P3W,Rs=16 Ω Ls = 0.2 7.5HP-DE	FXLMS	PI	PWM	DSTATCOM	[135]
Mitigation of current THD and provides load balancing along have been achieved under distorted load. Also, BESS has been found capable of providing active power.	3P3W, 3.7kW, 230V SyRG, 5.5kW, 415 V, AC drive	NN	PI	PWM	DSTATCOM	[136]
Elimination of current harmonics, load balancing along with controlled terminal voltage has been achieved under N-L load.	3P3W,3.7KW-PMSG	Adaline	PI	PWM	DSTATCOM	[121]
Compensation of the desired amount of reactive power has been achieved and maintained load balancing under N-L load.	3P3W, 3.7kW-SEIG, 230V	SMC	PI	HCC	DSTATCOM	[137]
Current harmonics has been mitigated with the maintaining UPF. Also, balancing loads and voltage regulation has been achieved with neutral current compensation under N-L loads.	3P4W, PV-4.5kW, PMSG -3.7kW, 230V, 400V Battery	Admittance based	PI	HCC	VSC	[138]
Voltage and frequency control, mitigation of PQ issues, the power balance in the whole system under various disturbances ranging from significant load variation to RES uncertainty have been achieved.	3P3W, SyRG-3.7kW, PV -OCV 350V, 400V Battery	Composite Observer	PI	HCC	VSC	[139]
The voltage differences between the bus and PCC of the droop controlled grid-connected (DCGC-MG) system decreased significantly. Thus, enhance PQ of the GCC has been achieved.	Grid Simulator, 650V DC, 311V MG, DCGCMG	Hierarchical theory (HT)	PI	-	VSC	[140]
The grid inverter guarantees uninterrupted electrical power supply has been achieved under power cuts or fluctuations.	WE-600W, PV-400W	PLL based	PI	-	H-Bridge	[141]

has been found comfortable with *R&D* controllers and output of these algorithms is superior compared to the conventional control algorithms. In addition to the above, the compatibility and performance of adaptive control algorithms with RE penetration provide better results compared to conventional control algorithms. The performance comparison of 3P3W and 3P4W system in an isolated mode, utility grid-connected mode and RE integrated mode is listed in Table 8, Table 9 and Table 10. The aim of these tables is incorporating recent research in the area of PQ mitigation. For this purpose, tabled data shows the system parameters, reference signal generation algorithms, voltage regulation devices, comparators for PWM generator, DFACTS devices used for the various researches in different applications. The performance of various control algorithms has also been discussed in the above mentioned Tables. Based rigorous state-of-the-art included in the revised version of the paper, critical factors are also investigated, which are important for future modern utility grid with RE penetration in terms of feasibility and economic considerations. These factors and their illustrations are presented in Table 11.

VI. LEARNING OUTCOMES AND RECOMMENDATION FOR FUTURE RESEARCH

The learning outcomes and recommendation for future research are as follows:

TABLE 9. Performance analysis of 3P3W and 3P4W utility grid with grid connected mode.

Achievements	System	RSGA	Regulator	Comparator	DFACTS devices	Ref.
Reactive power compensation and current harmonics have been mitigated. Also, the balancing of asymmetrical loads has been achieved under linear and non-linear (N-L) loads.	3P3W, 100V (L-L), 50Hz; Ls=5.8mH, Rs=3.6Ω	Vectorial-IRPT	PI	HCC	Hybrid power filter	[142]
Voltage regulation, reactive power and current harmonics have been mitigated. Also, it provides quick response and zero phase shifts along with reducing the computational complexity and cost of the DSTATCOM have been achieved under N-L loads.	3P4W, 110V (L-L), 50Hz; Ls=3.5mH, Rs=0.01Ω	Adaline based NN	PI	PWM	DSTATCOM	[109]
DC bus voltage and power factor have been maintained with load balancing under linear and N-L loads.	3P4W, 415V (L-L), 50Hz, Ls=2mH	Peak detection	PI	PWM	DSTATCOM	[143]
Compensate of the desired amount of reactive power, and mitigation of harmonics has been achieved under N-L loads.	3P3W, 4 KVA, 415V (L-L), 50Hz	Leaky-LMS	PI	PWM	DSTATCOM	[144]
Unity power factor has been maintained and compensate the reactive power to improve PQ under N-L load.	3P3W, 110V (L-L), 50Hz; Ls=3.2mH	EPLL	PI	PWM	DSTATCOM	[145]
Suppression of existing noises, fast convergence and neutral current compensation in the system has been achieved using Hyperbolic tangent function-least mean square (H-LMS).	3P4W, 220V (L-L), 50Hz	H-LMS	PI	HCC	DSTATCOM	[146]
Reactive power compensation and current harmonics have been mitigated. Also, the balancing of loads has been achieved under linear and N-L load.	3P3W, 110V (L-L), 50Hz; Ls=2mH, Rs=0.2Ω	Anti-Hebbian algorithm	-	PWM	DSTATCOM	[147]
Current harmonics has been mitigated with the maintaining UPF. Also, voltage regulation has been achieved under N-L load.	3P3W, 225V (L-L), 50Hz	Back Propagation	PI	PWM	DSTATCOM	[148]
Reactive power compensation and current harmonics have been mitigated using Adaptive synchronous extraction (ASE). Also, balancing of loads and voltage regulation has been achieved under linear and N-L load.	3P3W, 110V (L-L), 50Hz; Ls=2mH, small internal-R	ASE	PI	PWM	DSTATCOM	[149]
Self-supporting dc bus voltage has been achieved to maintained power quality using modified synchronous detection (MSD) under non-ideal ac mains and N-L load.	3P3W, 415V (L-L), 50Hz; Ls=2mH, Rs=0.07Ω	MSD	PI	PWM	DSTATCOM	[150]
Compensation of the desired amount of reactive power has been achieved using space vector modulation (SVM) under N-L load.	3P3W, 400V (L-L), 50Hz	SVM	-	HCC	DSTATCOM	[95]
Grid harmonics mitigation and compensation of excessive neutral current have been achieved under N-Load.	3P4W, 125V (L-L), 50Hz; Ls=3mH	Notch filter	PI	HCC	DSTATCOM	[151]
Reactive power compensation and harmonics have been mitigated using kernel incremental meta-learning algorithm (KIMEL).	3P3W, 415V (L-L), 50Hz; Ls=2.5mH	KIMEL-ICCT	PI	PWM	DSTATCOM	[152]
Reactive power compensation and current harmonics have been mitigated. Also, adaptive FL controller reduces the overshoot and undershoots and improve the response under unbalanced NLload and distorted supply voltage conditions.	3P3W, 415V (L-L), 50Hz	Self-Tuning Filter-IRPT	FL	PWM	DSTATCOM	[153]
Intrinsic mode functions in empirical mode decomposition (EMD) have been used for maintaining the efficiency of system.	3P3W, 100V (L-L), 50Hz	EMD	PI	HCC	SAPF	[154]

TABLE 10. Performance analysis of 3P3W and 3P4W utility grid with RE integrated mode.

Achievements	System	RSGA	Regulator	Comparator	DFACTS devices	Ref
Mitigation of various PQ issues under unbalanced NL-loads and supply active power as required has been achieved.	3P4W, PSMG-2.5KW, Grid-30V,60Hz	PLL based IRPT	PI	HCC	VSC	[93]
DC-link voltage has been maintained to control the power flow of SPV system by compensating reactive power under N-L load.	3P3W, PV Array Grid 230V, 50 Hz	SRF and IRPT	PI	SMC	DSTATCOM	[80]
The inverter is vigorously compensated the current imbalance harmonics and reactive power for smooth bidirectional power flow.	3P4W, PMSG-2.5KW, Grid 30V, 60Hz	ANFIS	PI	HCC	VSC	[83]
Smooth SPV-integration and balancing of loads have been achieved using Normalized-LMS (NLMS).	3P3W, SPV-8.1kW, Grid 415V, 50 Hz	NLMS	PI	PWM	VSC	[71]
Mitigation of various power quality issues under different dynamics and steady-state operating conditions have been achieved.	3P4W, SPV-30KW Grid 415V, 50Hz	ANF	PI	PWM	VSC	[78]
Harmonics elimination, PF correction, load balancing, voltage fluctuations, compensation of reactive power, under N-L loads have been achieved using variable step-size least mean fourth (VSS-LMF) algorithm.	3P3W, SPV-6.8kW Grid 415V, 50Hz	VSS-LMF	PI	PWM	VSC	[73]
Mitigation of harmonics, reactive power, and neutral current compensation have been achieved and maintain balanced grid currents using Second Order Generalized Integrator-Quadrature (SOGI-Q).	3P4W, SPV-7kW Grid 415V, 50Hz	SOGI-Q	PI	HCC	VSC	[155]
Power quality has been maintained at its desired level. Also, steady-state and dynamic changes in wind speeds are maintained.	3P4W, DFIG-3.7kW Grid 415V, 50Hz	PLL based	PI	PWM	VSC	[67]
Elimination of current harmonics and provides load balancing with controlled terminal voltage have been achieved.	3P3W, SPV-6.8kW, Grid 415V, 50Hz	PLL-less algorithm	PI	PWM	VSC	[156]
Compensate the various power quality issues such as reactive power under NL load using conservative power theory (CPT).	3P4W, PMSG-10KW Opal RT	CPT based dq frame	PI	SPWM	VSC	[157]
The need for additional power converters for PQ mitigation studies has been avoided by using the proposed structure. It has never been implemented before for RES application.	3P3W, RES inverter-5kVA, Grid 415V, 50Hz	ANF	PI	PWM	VSC	[158]
Various PQ issues have been mitigated, and the proposed system effectively transfers active power from the PV array to the local loads, and the grid using decorrelation normalized least mean square (DNLMS) algorithm.	3P3W, SPV-5.36kW Grid 227Vrms, 50Hz	DNLMS	PI	HCC	VSC	[22]
The LMF control is found more effective then LMS control in terms of minimization of mean square error and static error for PQ mitigation.	3P3W, SPV-8kW, Grid 415V, 50Hz.	LMF	PI	PWM	VSC	[114]
Low mean square error and converges faster along with improved PQ has been achieved.	3P4W, SPV-54kW, Grid 415V, 50Hz	Modified LMF	PI	PWM	VSC	[159]

- This review provides various concepts related to power quality and its standards in the area of RE penetration into the utility grid, which is useful for grid operators.
- This review provides the performance comparison of various DFACTS devices used to mitigate PQ in utility grids integrated with different RE sources. It also established that potential choice for the PQ mitigation under various conditions is DSTATCOM.
- This review also guides in selecting PQ mitigation method, DFACTS device based on the type of RE penetration and type of the AC grid.
- The beginners of this research area would have exposure to experimental architecture for RE penetration into 3P3W and 3P4W utility grid and DFACTS for PQ improvement.
- This review provides a broad classification of various control algorithms used for PQ mitigation based on conventional and adaptive control methodologies.
- It provides an insight into various aspects of a hardware implementation for control algorithms using different technologies such as FPGA, dSPACE.

A wide scope for future research in the PQ mitigation with RE penetration may include:

- A thorough investigation is required of various PQ issues in a utility grid with hybrid RE penetration of different combinations and levels.
- The performance of various adaptive control algorithms of RE sources with variations in the AC grid can be a potential future research topic.
- The investigation into the aspects of sustainability, reliability, cost, size, the weight of various DFACTS devices used for PQ mitigation into the utility grid with RE penetration may be considered as a future research topic.

VII. CONCLUSION

A comprehensive state of the art for different implemented control algorithms to enhance the power quality in 3P3W and 3P4W utility grid with RE penetration has been critically reviewed. The international research status with the details related to design aspects of various control algorithms both in simulation and experimental studies have been presented. The performance of various algorithms is summarized for

guidance. The research beginners in this area would be able to select the topology and control algorithm based on the grid configuration. The technical details of the hardware used for experimental work are also provided in the view of benefiting the designers and researchers in the field of PQ mitigation in the utility grid with RE penetration. A learning outcome of this review and the possible scope of future work have been highlighted. Authors hope that this review will pave the way for new ideas in the implementation of PQ mitigation algorithms in association with DFACTS devices thereby enhancing the RE penetration level for promotion of the green energy.

REFERENCES

[1] O. Ellabban, H. Abu-Rub, and F. Blaabjerg, "Renewable energy resources: Current status, future prospects and their enabling technology," *Renew. Sustain. Energy Rev.*, vol. 39, pp. 748–764, Nov. 2014.
[2] F. Blaabjerg and K. Ma, "Future on power electronics for wind turbine systems," *IEEE J. Emerg. Sel. Topics Power Electron.*, vol. 1, no. 3, pp. 139–152, Sep. 2013.
[3] A. M. Foley, B. P. Ó. Gallachóir, E. J. McKeogh, D. Milborrow, and P. G. Leahy, "Addressing the technical and market challenges to high wind power integration in Ireland," *Renew. Sustain. Energy Rev.*, vol. 19, pp. 692–703, Mar. 2013.
[4] *Global Energy Transformation: A Roadmap to 2050*, IRENA, Abu Dhabi, United Arab Emirates, 2019.
[5] M. H. Bollen, *Understanding Power Quality Problems*, vol. 3. Piscataway, NJ, USA: IEEE Press, 2013, pp. 1–35.
[6] E. Hossain, M. R. Tur, S. Padmanaban, S. Ay, and I. Khan, "Analysis and mitigation of power quality issues in distributed generation systems using custom power devices," *IEEE Access*, vol. 6, pp. 16816–16833, 2018.
[7] O. P. Mahela and A. G. Shaik, "A review of distribution static compensator," *Renew. Sustain. Energy Rev.*, vol. 50, pp. 531–546, Oct. 2015.
[8] H. Akagi, "Active harmonic filters," *Proc. IEEE*, vol. 93, no. 12, pp. 2128–2141, Dec. 2005.
[9] D. Sreenivasarao, P. Agarwal, and B. Das, "Neutral current compensation in three-phase, four-wire systems: A review," *Electr. Power Syst. Res.*, vol. 86, pp. 170–180, May 2012.
[10] G. W. Chang and N. Cong Chinh, "Coyote optimization algorithm-based approach for strategic planning of photovoltaic distributed generation," *IEEE Access*, vol. 8, pp. 36180–36190, 2020.
[11] O. P. Mahela, N. Gupta, M. Khosravy, and N. Patel, "Comprehensive overview of low voltage ride through methods of grid integrated wind generator," *IEEE Access*, vol. 7, pp. 99299–99326, 2019.
[12] R. W. Mosobi, T. Chichi, and S. Gao, "Modeling and power quality analysis of integrated renewable energy system," in *Proc. 18th Nat. Power Syst. Conf. (NPSC)*, Dec. 2014, pp. 1–6.
[13] Z. Tang, M. Su, Y. Sun, B. Cheng, Y. Yang, F. Blaabjerg, and L. Wang, "Hybrid UP-PWM scheme for HERIC inverter to improve power quality and efficiency," *IEEE Trans. Power Electron.*, vol. 34, no. 5, pp. 4292–4303, May 2019.
[14] J. M. Carrasco, L. G. Franquelo, J. T. Bialasiewicz, E. Galván, R. C. PortilloGuisado, M. A. M. Prats, J. I. Leon, and N. Moreno-Alfonso, "Power-electronic systems for the grid integration of renewable energy sources: A survey," *IEEE Trans. Ind. Electron.*, vol. 53, no. 4, pp. 1002–1016, Jun. 2006.
[15] G. Tsengenes and G. Adamidis, "Investigation of the behavior of a three phase grid-connected photovoltaic system to control active and reactive power," *Electr. Power Syst. Res.*, vol. 81, no. 1, pp. 177–184, 2011.
[16] O. P. Mahela and A. G. Shaik, "Power quality improvement in distribution network using DSTATCOM with battery energy storage system," *Int. J. Electr. Power Energy Syst.*, vol. 83, pp. 229–240, Dec. 2016.
[17] B. Singh, "Recent trends in power quality improvements techniques," in *Proc. 7th Int. Conf. Power Electron. Drive Syst.*, Nov. 2007, pp. 1–155.
[18] B. Han, B. Bae, H. Kim, and S. Baek, "Combined operation of unified power-quality conditioner with distributed generation," *IEEE Trans. Power Del.*, vol. 21, no. 1, pp. 330–338, Jan. 2006.
[19] H. Hafezi and R. Faranda, "Dynamic voltage conditioner: A new concept for smart low-voltage distribution systems," *IEEE Trans. Power Electron.*, vol. 33, no. 9, pp. 7582–7590, Sep. 2018.
[20] A. Ghosh and G. Ledwich, *Power Quality Enhancement Using Custom Power Devices*. Amsterdam, The Netherlands: Elsevier, 2012.
[21] O. P. Mahela and A. G. Shaik, "Topological aspects of power quality improvement techniques: A comprehensive overview," *Renew. Sustain. Energy Rev.*, vol. 58, pp. 1129–1142, May 2016.
[22] S. Pradhan, I. Hussain, B. Singh, and B. K. Panigrahi, "Performance improvement of grid-integrated solar PV system using DNLMS control algorithm," *IEEE Trans. Ind. Appl.*, vol. 55, no. 1, pp. 78–91, Jan. 2019.
[23] H. Akagi, E. H. Watanabe, and M. Aredes, *Instantaneous Power Theory and Applications to Power Conditioning*, vol. 62. Hoboken, NJ, USA: Wiley, 2017.
[24] R. S. Herrera, P. Salmerón, and H. Kim, "Instantaneous reactive power theory applied to active power filter compensation: Different approaches, assessment, and experimental results," *IEEE Trans. Ind. Electron.*, vol. 55, no. 1, pp. 184–196, Jan. 2008.
[25] S. Bhattacharya and D. Divan, "Synchronous frame based controller implementation for a hybrid series active filter system," in *Proc. Conf. Rec. IEEE Ind. Appl. Conf., 13th IAS Annu. Meeting (IAS)*, vol. 3, Oct. 1995, pp. 2531–2540.
[26] B. Singh and V. Verma, "Selective compensation of power-quality problems through active power filter by current decomposition," *IEEE Trans. Power Del.*, vol. 23, no. 2, pp. 792–799, Apr. 2008.
[27] G. S. Chawda and A. G. Shaik, "Fuzzy logic based control algorithm for DSTATCOM connected to weak AC grid," in *Proc. 2nd Int. Conf. Power, Energy Environ., Towards Smart Technol. (ICEPE)*, Jun. 2018, pp. 1–6.
[28] Z. Shu, Y. Guo, and J. Lian, "Steady-state and dynamic study of active power filter with efficient FPGA-based control algorithm," *IEEE Trans. Ind. Electron.*, vol. 55, no. 4, pp. 1527–1536, Apr. 2008.
[29] K.-K. Shyu, M.-J. Yang, Y.-M. Chen, and Y.-F. Lin, "Model reference adaptive control design for a shunt Active-Power-Filter system," *IEEE Trans. Ind. Electron.*, vol. 55, no. 1, pp. 97–106, Jan. 2008.
[30] G. S. Chawda and A. G. Shaik, "Smooth grid synchronization in weak AC grid with high wind energy penetration using distribution static compensator," in *Proc. 2nd Int. Conf. Smart Grid Renew. Energy (SGRE)*, Nov. 2019, pp. 1–6.
[31] B. Singh and J. Solanki, "An implementation of an adaptive control algorithm for a three-phase shunt active filter," *IEEE Trans. Ind. Electron.*, vol. 56, no. 8, pp. 2811–2820, Aug. 2009.
[32] B. Singh and J. Solanki, "A comparative study of control algorithms for DSTATCOM for load compensation," in *Proc. IEEE Int. Conf. Ind. Technol.*, Dec. 2006, pp. 1492–1497.
[33] M. Badoni, B. Singh, and A. Singh, "Adaptive recursive inverse-based control algorithm for shunt active power filter," *IET Power Electron.*, vol. 9, no. 5, pp. 1053–1064, Apr. 2016.
[34] B. Widrow, J. McCool, and M. Ball, "The complex LMS algorithm," *Proc. IEEE*, vol. 63, no. 4, pp. 719–720, Apr. 1975.
[35] V. L. Srinivas, S. Kumar, B. Singh, and S. Mishra, "Partially decoupled adaptive filter based multifunctional three-phase GPV system," *IEEE Trans. Sustain. Energy*, vol. 9, no. 1, pp. 311–320, Jan. 2018.
[36] P. Shah, I. Hussain, and B. Singh, "A novel fourth-order generalized integrator based control scheme for multifunctional SECS in the distribution system," *IEEE Trans. Energy Convers.*, vol. 33, no. 3, pp. 949–958, Sep. 2018.
[37] B. Singh, A. Chandra, and K. Al-Haddad, *Power Quality: Problems and Mitigation Techniques*. Hoboken, NJ, USA: Wiley, 2014.
[38] R. C. Dugan, M. F. McGranaghan, H. W. Beaty, and S. Santoso, *Electrical Power Systems Quality*, vol. 2. New York, NY, USA: McGraw-Hill, 1996.
[39] B. Singh, K. Al-Haddad, and A. Chandra, "A review of active filters for power quality improvement," *IEEE Trans. Ind. Electron.*, vol. 46, no. 5, pp. 960–971, Oct. 1999.
[40] H. J. Green and T. Wind, "The IEEE grid interconnection standard: How will it affect wind power?" Nat. Renew. Energy Lab., Golden, CO, USA, Tech. Rep. NREL/CP-500-28409, 2000.
[41] X. Liang, "Emerging power quality challenges due to integration of renewable energy sources," *IEEE Trans. Ind. Appl.*, vol. 53, no. 2, pp. 855–866, Mar. 2017.
[42] *1159-2009. IEEE Recommended Practice for Monitoring Electric Power Quality Industrial and Commercial Applications*, Inst. Elect. Electron. Eng., New York, NY, USA, 2009. [Online]. Available: http://www.coe.ufrj.br/~richard/Acionamentos/IEEE519.pdf
[43] T.-F. Wu, C.-H. Chang, L.-C. Lin, and C.-L. Kuo, "Power loss comparison of single-and two-stage grid-connected photovoltaic systems," *IEEE Trans. Energy Convers.*, vol. 26, no. 2, pp. 707–715, Jun. 2011.

[44] T. M. Blooming and D. J. Carnovale, "Application of IEEE STD 519-1992 harmonic limits," in *Proc. Conf. Rec. Annu. Pulp Paper Ind. Tech. Conf.*, 2006, pp. 1–9.

[45] I. F. II, *IEEE Recommended Practices and Requirements for Harmonic Control in Electrical Power Systems*, IEEE Standard 519-2014 (Revision of IEEE Std 519-1992), New York, NY, USA, 1993, p. 1. [Online]. Available: https://edisciplinas.usp.br/pluginfile.php/1589263/mod_resource/content/1/IEE%20Std%20519-2014.pdf

[46] T. S. Basso and R. D. DeBlasio, "IEEE P1547-series of standards for interconnection," in *Proc. IEEE PES Transmiss. Distrib. Conf. Exposit.*, vol. 2, Sep. 2003, pp. 556–561.

[47] *IEEE Recommended Practice and Requirements for Harmonic Control in Electric Power Systems*, IEEE Standard 519-2014, (Revision IEEE Std 519-1992), 2014, pp. 1–29.

[48] D. D. Sabin and A. Sannino, "A summary of the draft IEEE P1409 custom power application guide," in *Proc. Transmiss. Distrib. Conf. Exposit. (PES)*, vol. 3, Sep. 2003, pp. 931–936.

[49] K. M. Muttaqi, J. Aghaei, V. Ganapathy, and A. E. Nezhad, "Technical challenges for electric power industries with implementation of distribution system automation in smart grids," *Renew. Sustain. Energy Rev.*, vol. 46, pp. 129–142, Jun. 2015.

[50] P. S. Georgilakis and N. D. Hatziargyriou, "A review of power distribution planning in the modern power systems era: Models, methods and future research," *Electr. Power Syst. Res.*, vol. 121, pp. 89–100, Apr. 2015.

[51] C. Chakraborty, H. H.-C. Iu, and D. D.-C. Lu, "Power converters, control, and energy management for distributed generation," *IEEE Trans. Ind. Electron.*, vol. 62, no. 7, pp. 4466–4470, Jul. 2015.

[52] D. M. Divan, W. E. Brumsickle, R. S. Schneider, B. Kranz, R. W. Gascoigne, D. T. Bradshaw, M. R. Ingram, and I. S. Grant, "A distributed static series compensator system for realizing active power flow control on existing power lines," *IEEE Trans. Power Del.*, vol. 22, no. 1, pp. 642–649, Jan. 2007.

[53] F. H. Gandoman, A. Ahmadi, A. M. Sharaf, P. Siano, J. Pou, B. Hredzak, and V. G. Agelidis, "Review of FACTS technologies and applications for power quality in smart grids with renewable energy systems," *Renew. Sustain. Energy Rev.*, vol. 82, pp. 502–514, Feb. 2018.

[54] E. Acha, C. R. Fuerte-Esquivel, H. Ambriz-Perez, and C. Angeles-Camacho, *FACTS: Modelling and Simulation in Power Networks*. Hoboken, NJ, USA: Wiley, 2004.

[55] N. G. Hingorani, L. Gyugyi, and M. El-Hawary, *Understanding FACTS: Concepts and Technology of Flexible AC Transmission Systems*, vol. 1. New York, NY, USA: IEEE Press, 2000.

[56] B. Mahdad, "Optimal power flow with consideration of FACTS devices using genetic algorithm: Application to the Algerian network," Ph.D. dissertation, Univ. Mohamed Khider Biskra, Biskra, Algeria, Sep. 2010.

[57] H. Vallecha, "Smart utilization of solar and wind power farm inverters as SSSC in grid connected renewable energy system," in *Proc. IEEE 6th Int. Conf. Power Syst. (ICPS)*, Mar. 2016, pp. 1–5.

[58] A. Edris, "Proposed terms and definitions for flexible AC transmission system (FACTS)," *IEEE Trans. Power Del.*, vol. 12, no. 4, p. 1, Oct. 1997.

[59] K. K. Prasad, H. Myneni, and G. S. Kumar, "Power quality improvement and PV power injection by DSTATCOM with variable DC link voltage control from RSC-MLC," *IEEE Trans. Sustain. Energy*, vol. 10, no. 2, pp. 876–885, Apr. 2019.

[60] D. Li and Z. Q. Zhu, "A novel integrated power quality controller for microgrid," *IEEE Trans. Ind. Electron.*, vol. 62, no. 5, pp. 2848–2858, May 2015.

[61] S. Devassy and B. Singh, "Control of solar photovoltaic integrated UPQC operating in polluted utility conditions," *IET Power Electron.*, vol. 10, no. 12, pp. 1413–1421, Oct. 2017.

[62] R. K. Varma, S. Auddy, and Y. Semsedini, "Mitigation of subsynchronous resonance in a series-compensated wind farm using FACTS controllers," *IEEE Trans. Power Del.*, vol. 23, no. 3, pp. 1645–1654, Jul. 2008.

[63] Y. Xiao, Y. H. Song, and Y. Z. Sun, "Power flow control approach to power systems with embedded FACTS devices," *IEEE Trans. Power Syst.*, vol. 17, no. 4, pp. 943–950, Nov. 2002.

[64] P. De Martini, "Operational coordination architecture: New models and approaches," *IEEE Power Energy Mag.*, vol. 17, no. 5, pp. 29–39, Sep. 2019.

[65] S. Peyghami, P. Davari, M. Fotuhi-Firuzabad, and F. Blaabjerg, "Standard test systems for modern power system analysis: An overview," *IEEE Ind. Electron. Mag.*, vol. 13, no. 4, pp. 86–105, Dec. 2019.

[66] N. K. S. Naidu and B. Singh, "Grid-interfaced DFIG-based variable speed wind energy conversion system with power smoothening," *IEEE Trans. Sustain. Energy*, vol. 8, no. 1, pp. 51–58, Jan. 2017.

[67] R. K. Agarwal, I. Hussain, and B. Singh, "Integration of single-stage SPV generation to three-phase distribution grid using a variable step size LMS control technique," in *Proc. IEEE 1st Int. Conf. Power Electron., Intell. Control Energy Syst. (ICPEICES)*, Jul. 2016, pp. 1–6.

[68] M. Badoni, A. Singh, and B. Singh, "Adaptive neurofuzzy inference system least-mean-square-based control algorithm for DSTATCOM," *IEEE Trans. Ind. Informat.*, vol. 12, no. 2, pp. 483–492, Apr. 2016.

[69] P. Shah, I. Hussain, B. Singh, A. Chandra, and K. Al-Haddad, "GI-based control scheme for single-stage grid interfaced SECS for power quality improvement," *IEEE Trans. Ind. Appl.*, vol. 55, no. 1, pp. 869–881, Jan. 2019.

[70] R. K. Agarwal, I. Hussain, and B. Singh, "Grid integration of single stage SPV system using NLMS filtering control technique," in *Proc. IEEE 6th Int. Conf. Power Syst. (ICPS)*, Mar. 2016, pp. 1–6.

[71] R. K. Agarwal, I. Hussain, and B. Singh, "Implementation of LLMF control algorithm for three-phase grid-tied SPV-DSTATCOM system," *IEEE Trans. Ind. Electron.*, vol. 64, no. 9, pp. 7414–7424, Sep. 2017.

[72] R. K. Agarwal, I. Hussain, B. Singh, A. Chandra, and K. Al-Haddad, "A multifunctional three-phase grid-connected single-stage SPV system using an intelligent adaptive control technique," in *Proc. IECON - 42nd Annu. Conf. IEEE Ind. Electron. Soc.*, Oct. 2016, pp. 3000–3005.

[73] N. Beniwal, I. Hussain, and B. Singh, "Second-order Volterra-filter-based control of a solar PV-DSTATCOM system to achieve Lyapunov's stability," *IEEE Trans. Ind. Appl.*, vol. 55, no. 1, pp. 670–679, Jan. 2019.

[74] I. Hussain, M. Kandpal, and B. Singh, "Real-time implementation of three-phase single-stage SPV grid-tied system using TL-VSC," *IET Renew. Power Gener.*, vol. 11, no. 12, pp. 1576–1583, Oct. 2017.

[75] M. Patowary, G. Panda, B. R. Naidu, and B. C. Deka, "ANN-based adaptive current controller for on-grid DG system to meet frequency deviation and transient load challenges with hardware implementation," *IET Renew. Power Gener.*, vol. 12, no. 1, pp. 61–71, Jan. 2018.

[76] P. Shah, I. Hussain, and B. Singh, "Fuzzy logic based FOGI-FLL algorithm for optimal operation of single-stage three-phase grid interfaced multifunctional SECS," *IEEE Trans. Ind. Informat.*, vol. 14, no. 8, pp. 3334–3346, Aug. 2018.

[77] B. Singh, C. Jain, S. Goel, A. Chandra, and K. Al-Haddad, "A multifunctional grid-tied solar energy conversion system with ANF-based control approach," *IEEE Trans. Ind. Appl.*, vol. 52, no. 5, pp. 3663–3672, Sep. 2016.

[78] S. Kumar and B. Singh, "A multipurpose PV system integrated to a three-phase distribution system using an LWDF-based approach," *IEEE Trans. Power Electron.*, vol. 33, no. 1, pp. 739–748, Jan. 2018.

[79] S. Mishra and P. K. Ray, "Nonlinear modeling and control of a photovoltaic fed improved hybrid DSTATCOM for power quality improvement," *Int. J. Electr. Power Energy Syst.*, vol. 75, pp. 245–254, Feb. 2016.

[80] Y. Shan, J. Hu, K. W. Chan, Q. Fu, and J. M. Guerrero, "Model predictive control of bidirectional DC–DC converters and AC/DC interlinking Converters—A new control method for PV-Wind-Battery microgrids," *IEEE Trans. Sustain. Energy*, vol. 10, no. 4, pp. 1823–1833, Oct. 2019.

[81] B. Singh and S. Kumar, "Grid integration of 3P4W solar PV system using M-LWDF-based control technique," *IET Renew. Power Gener.*, vol. 11, no. 8, pp. 1174–1181, Jun. 2017.

[82] M. Singh and A. Chandra, "Real-time implementation of ANFIS control for renewable interfacing inverter in 3P4W distribution network," *IEEE Trans. Ind. Electron.*, vol. 60, no. 1, pp. 121–128, Jan. 2013.

[83] P. J. Chauhan and J. K. Chatterjee, "A novel speed adaptive stator current compensator for voltage and frequency control of standalone SEIG feeding three-phase four-wire system," *IEEE Trans. Sustain. Energy*, vol. 10, no. 1, pp. 248–256, Jan. 2019.

[84] S. Kumar and B. Singh, "Multi-objective single-stage SPV system integrated to 3P4W distribution network using DMSI-based control technique," *IEEE Trans. Ind. Appl.*, vol. 54, no. 3, pp. 2656–2664, May 2018.

[85] M.-J. Tsai, H.-C. Chen, and P.-T. Cheng, "Eliminating the neutral-point oscillation of the four-wire NPC active power filter," *IEEE Trans. Power Electron.*, vol. 34, no. 7, pp. 6233–6240, Jul. 2019.

[86] S. Beheshtaein, M. Savaghebi, R. M. Cuzner, S. Golestan, and J. M. Guerrero, "Modified secondary-control-based fault current limiter for inverters," *IEEE Trans. Ind. Electron.*, vol. 66, no. 6, pp. 4798–4804, Jun. 2019.

[87] F. H. Md Rafi, M. J. Hossain, G. Town, and J. Lu, "Smart voltage-source inverters with a novel approach to enhance neutral-current compensation," *IEEE Trans. Ind. Electron.*, vol. 66, no. 5, pp. 3518–3529, May 2019.
[88] Y. Fu, Y. Li, Y. Huang, X. Lu, K. Zou, C. Chen, and H. Bai, "Imbalanced load regulation based on virtual resistance of a three-phase four-wire inverter for EV vehicle-to-home applications," *IEEE Trans. Transport. Electrific.*, vol. 5, no. 1, pp. 162–173, Mar. 2019.
[89] A. Hintz, U. R. Prasanna, and K. Rajashekara, "Comparative study of the three-phase grid-connected inverter sharing unbalanced three-phase and/or single-phase systems," *IEEE Trans. Ind. Appl.*, vol. 52, no. 6, pp. 5156–5164, Nov. 2016.
[90] P. Jayaprakash, B. Singh, and D. P. Kothari, "DSP based implementation of a three-phase four-wire DSTATCOM for voltage regulation and power quality improvement," in *Proc. 35th Annu. Conf. IEEE Ind. Electron.*, Nov. 2009, pp. 3660–3665.
[91] J. Borkowski, D. Kania, and J. Mroczka, "Interpolated-DFT-based fast and accurate frequency estimation for the control of power," *IEEE Trans. Ind. Electron.*, vol. 61, no. 12, pp. 7026–7034, Dec. 2014.
[92] M. Singh, V. Khadkikar, A. Chandra, and R. K. Varma, "Grid interconnection of renewable energy sources at the distribution level with power-quality improvement features," *IEEE Trans. Power Del.*, vol. 26, no. 1, pp. 307–315, Jan. 2011.
[93] B. Singh and J. Solanki, "A comparison of control algorithms for DSTATCOM," *IEEE Trans. Ind. Electron.*, vol. 56, no. 7, pp. 2738–2745, Jul. 2009.
[94] K. Murugesan, R. Muthu, S. Vijayenthiran, and J. Mervin, "Prototype hardware realization of the DSTATCOM for reactive power compensation," *Int. J. Electr. Power Energy Syst.*, vol. 65, pp. 169–178, Feb. 2015.
[95] B. Singh, A. Adya, A. P. Mittal, and J. R. P. Gupta, "Application of battery energy operated system to isolated power distribution systems," in *Proc. 7th Int. Conf. Power Electron. Drive Syst.*, Nov. 2007, pp. 526–532.
[96] R. S. Bhatia, S. P. Jain, D. Kumar Jain, and B. Singh, "Battery energy storage system for power conditioning of renewable energy sources," in *Proc. Int. Conf. Power Electron. Drives Syst.*, Nov. 2005, pp. 501–506.
[97] L. B. G. Campanhol, S. A. O. da Silva, A. A. de Oliveira, and V. D. Bacon, "Power flow and stability analyses of a multifunctional distributed generation system integrating a photovoltaic system with unified power quality conditioner," *IEEE Trans. Power Electron.*, vol. 34, no. 7, pp. 6241–6256, Jul. 2019.
[98] B. Singh, P. Jayaprakash, and D. P. Kothari, "New control approach for capacitor supported DSTATCOM in three-phase four wire distribution system under non-ideal supply voltage conditions based on synchronous reference frame theory," *Int. J. Electr. Power Energy Syst.*, vol. 33, no. 5, pp. 1109–1117, Jun. 2011.
[99] A. K. Verma, B. Singh, and D. T. Shahani, "Grid interfaced solar photovoltaic power generating system with power quality improvement at AC mains," in *Proc. IEEE 3rd Int. Conf. Sustain. Energy Technol. (ICSET)*, Sep. 2012, pp. 177–182.
[100] J. Philip, C. Jain, K. Kant, B. Singh, S. Mishra, A. Chandra, and K. Al- Haddad, "Control and implementation of a standalone solar photovoltaic hybrid system," in *Proc. IEEE Ind. Appl. Soc. Annu. Meeting*, Oct. 2015, pp. 1–8.
[101] Y. Singh, I. Hussain, B. Singh, and S. Mishra, "Single-phase single-stage grid tied solar PV system with active power filtering using power balance theory," *J. Inst. Eng., India B*, vol. 99, no. 3, pp. 301–311, Jun. 2018.
[102] N. R. Tummuru, M. K. Mishra, and S. Srinivas, "Multifunctional VSC controlled microgrid using instantaneous symmetrical components theory," *IEEE Trans. Sustain. Energy*, vol. 5, no. 1, pp. 313–322, Jan. 2014.
[103] Y. Xu, C. Ma, L. Yang, Z. Gong, H. Pu, and Z. Zhang, "Study on sliding mode control with RBF network for DSTATCOM," in *Proc. Int. Conf. E-Product E-Service E-Entertainment*, Nov. 2010, pp. 7394–7399.
[104] N. K. Kummari, A. K. Singh, and P. Kumar, "Comparative evaluation of DSTATCOM control algorithms for load compensation," in *Proc. IEEE 15th Int. Conf. Harmon. Qual. Power*, Jun. 2012, pp. 299–306.
[105] B. Singh, S. S. Murthy, and S. Gupta, "Analysis and design of STATCOM-based voltage regulator for self-excited induction generators," *IEEE Trans. Energy Convers.*, vol. 19, no. 4, pp. 783–790, Dec. 2004.
[106] D. Voglitsis, N. P. Papanikolaou, and A. C. Kyritsis, "Active cross-correlation anti-islanding scheme for PV module-integrated converters in the prospect of high penetration levels and weak grid conditions," *IEEE Trans. Power Electron.*, vol. 34, no. 3, pp. 2258–2274, Mar. 2019.
[107] B. Widrow, J. M. McCool, M. G. Larimore, and C. R. Johnson, "Stationary and nonstationary learning characteristics of the LMS adaptive filter," *Proc. IEEE*, vol. 64, no. 8, pp. 1151–1162, Aug. 1976.
[108] B. Singh, P. Jayaprakash, S. Kumar, and D. P. Kothari, "Implementation of neural-network-controlled three-leg VSC and a transformer as three-phase four-wire DSTATCOM," *IEEE Trans. Ind. Appl.*, vol. 47, no. 4, pp. 1892–1901, Jul. 2011.
[109] G. S. Chawda and A. G. Shaik, "Performance evaluation of adaline controlled dstatcom for multifarious load in weak AC grid," in *Proc. IEEE PES GTD Grand Int. Conf. Exposit. Asia (GTD Asia)*, Mar. 2019, pp. 356–361.
[110] M. U. Otaru, A. Zerguine, and L. Cheded, "Channel equalization using simplified least mean-fourth algorithm," *Digit. Signal Process.*, vol. 21, no. 3, pp. 447–465, May 2011.
[111] A. E.-S. El-Mahdy, "Adaptive channel estimation and equalization for rapidly mobile communication channels," *IEEE Trans. Commun.*, vol. 52, no. 7, pp. 1126–1135, Jul. 2004.
[112] E. Eweda, "Global stabilization of the least mean fourth algorithm," *IEEE Trans. Signal Process.*, vol. 60, no. 3, pp. 1473–1477, Dec. 2012.
[113] R. K. Agarwal, I. Hussain, and B. Singh, "LMF-based control algorithm for single stage three-phase grid integrated solar PV system," *IEEE Trans. Sustain. Energy*, vol. 7, no. 4, pp. 1379–1387, Oct. 2016.
[114] G. Gui, W. Peng, and F. Adachi, "Adaptive system identification using robust LMS/F algorithm," *Int. J. Commun. Syst.*, vol. 27, no. 11, pp. 2956–2963, Nov. 2014.
[115] S. S. Haykin, *Adaptive Filter Theory*. London, U.K.: Pearson, 2008.
[116] C. Paleologu, J. Benesty, and S. Ciochina, "A robust variable forgetting factor recursive least-squares algorithm for system identification," *IEEE Signal Process. Lett.*, vol. 15, pp. 597–600, Oct. 2008. [Online]. Available: https://ieeexplore.ieee.org/document/4639569
[117] S. C. Chan and Y. J. Chu, "A new state-regularized QRRLS algorithm with a variable forgetting factor," *IEEE Trans. Circuits Syst. II, Exp. Briefs*, vol. 59, no. 3, pp. 183–187, Mar. 2012.
[118] M. Badoni, A. Singh, and B. Singh, "Variable forgetting factor recursive least square control algorithm for DSTATCOM," *IEEE Trans. Power Del.*, vol. 30, no. 5, pp. 2353–2361, Oct. 2015.
[119] S.-H. Leung and C. F. So, "Gradient-based variable forgetting factor RLS algorithm in time-varying environments," *IEEE Trans. Signal Process.*, vol. 53, no. 8, pp. 3141–3150, Aug. 2005.
[120] B. Singh and R. Niwas, "Power quality improvement of PMSG-based DG set feeding three-phase loads," *IEEE Trans. Ind. Appl.*, vol. 52, no. 1, pp. 466–471, Jan. 2016.
[121] P. Garanayak, R. T. Naayagi, and G. Panda, "A high-speed master-slave ADALINE for accurate power system harmonic and inter-harmonic estimation," *IEEE Access*, vol. 8, pp. 51918–51932, 2020.
[122] B. Singh, V. Verma, and J. Solanki, "Neural network-based selective compensation of current quality problems in distribution system," *IEEE Trans. Ind. Electron.*, vol. 54, no. 1, pp. 53–60, Feb. 2007.
[123] B. Singh, S. K. Dube, S. R. Arya, A. Chandra, and K. Al-Haddad, "A comparative study of adaptive control algorithms in distribution static compensator," in *Proc. 39th Annu. Conf. IEEE Ind. Electron. Soc. (IECON)*, Nov. 2013, pp. 145–150.
[124] M. Badoni, A. Singh, and B. Singh, "Comparative performance of Wiener filter and adaptive least mean square-based control for power quality improvement," *IEEE Trans. Ind. Electron.*, vol. 63, no. 5, pp. 3028–3037, May 2016.
[125] S. Singh, S. Kewat, B. Singh, and B. K. Panigrahi, "Enhanced momentum LMS-based control technique for grid-tied solar system," *IET Power Electron.*, Feb. 2020. [Online]. Available: https://digital-library.theiet.org/content/journals/10.1049/iet-pel.2019.1126
[126] R. K. Agarwal, I. Hussain, and B. Singh, "Application of LMS-based NN structure for power quality enhancement in a distribution network under abnormal conditions," *IEEE Trans. Neural Netw. Learn. Syst.*, vol. 29, no. 5, pp. 1598–1607, May 2018.
[127] M. Fallah, H. M. Kojabadi, and F. Blaabjerg, "New control method for VSC-MTDC stations in the abnormal conditions of power system," *Control Eng. Pract.*, vol. 96, Mar. 2020, Art. no. 104316.
[128] M. I. Marei, E. F. El-Saadany, and M. M. A. Salama, "A flexible DG interface based on a new RLS algorithm for power quality improvement," *IEEE Syst. J.*, vol. 6, no. 1, pp. 68–75, Mar. 2012.
[129] M. Beza and M. Bongiorno, "An adaptive power oscillation damping controller by STATCOM with energy storage," *IEEE Trans. Power Syst.*, vol. 30, no. 1, pp. 484–493, Jan. 2015.

[130] V. L. Srinivas, S. Kumar, B. Singh, and S. Mishra, "A multifunctional GPV system using adaptive observer based harmonic cancellation technique," *IEEE Trans. Ind. Electron.*, vol. 65, no. 2, pp. 1347–1357, Feb. 2018.

[131] A. B. Shitole, H. M. Suryawanshi, G. G. Talapur, S. Sathyan, M. S. Ballal, V. B. Borghate, M. R. Ramteke, and M. A. Chaudhari, "Grid interfaced distributed generation system with modified current control loop using adaptive synchronization technique," *IEEE Trans. Ind. Informat.*, vol. 13, no. 5, pp. 2634–2644, Oct. 2017.

[132] B. Singh and V. Rajagopal, "Neural-network-based integrated electronic load controller for isolated asynchronous generators in small hydro generation," *IEEE Trans. Ind. Electron.*, vol. 58, no. 9, pp. 4264–4274, Sep. 2011.

[133] S. R. Arya, B. Singh, R. Niwas, A. Chandra, and K. Al-Haddad, "Power quality enhancement using DSTATCOM in distributed power generation system," *IEEE Trans. Ind. Appl.*, vol. 52, no. 6, pp. 5203–5212, Nov. 2016.

[134] R. Niwas and B. Singh, "Solid-state control for reactive power compensation and power quality improvement of wound field synchronous generator-based diesel generator sets," *IET Electr. Power Appl.*, vol. 9, no. 6, pp. 397–404, Jul. 2015.

[135] S. R. Arya, R. Niwas, K. Kant Bhalla, B. Singh, A. Chandra, and K. Al-Haddad, "Power quality improvement in isolated distributed power generating system using DSTATCOM," *IEEE Trans. Ind. Appl.*, vol. 51, no. 6, pp. 4766–4774, Nov. 2015.

[136] V. C. Sekhar, K. Kant, and B. Singh, "DSTATCOM supported induction generator for improving power quality," *IET Renew. Power Gener.*, vol. 10, no. 4, pp. 495–503, Apr. 2016.

[137] J. Philip, C. Jain, K. Kant, B. Singh, S. Mishra, A. Chandra, and K. Al-Haddad, "Control and implementation of a standalone solar photovoltaic hybrid system," *IEEE Trans. Ind. Appl.*, vol. 52, no. 4, pp. 3472–3479, Jul. 2016.

[138] K. Kant, C. Jain, and B. Singh, "A hybrid diesel-wind–PV-based energy generation system with brushless generators," *IEEE Trans. Ind. Informat.*, vol. 13, no. 4, pp. 1714–1722, Aug. 2017.

[139] W. Feng, K. Sun, Y. Guan, J. M. Guerrero, and X. Xiao, "Active power quality improvement strategy for grid-connected microgrid based on hierarchical control," *IEEE Trans. Smart Grid*, vol. 9, no. 4, pp. 3486–3495, Jul. 2018.

[140] M. Dali, J. Belhadj, and X. Roboam, "Hybrid solar–wind system with battery storage operating in grid-connected and standalone mode: Control and energy management—Experimental investigation," *Energy*, vol. 35, no. 6, pp. 2587–2595, Jun. 2010.

[141] P. Salmeron and S. P. Litran, "Improvement of the electric power quality using series active and shunt passive filters," *IEEE Trans. Power Del.*, vol. 25, no. 2, pp. 1058–1067, Apr. 2010.

[142] B. Singh, S. R. Arya, and C. Jain, "Simple peak detection control algorithm of distribution static compensator for power quality improvement," *IET Power Electron.*, vol. 7, no. 7, pp. 1736–1746, Jul. 2014.

[143] S. R. Arya and B. Singh, "Performance of DSTATCOM using leaky LMS control algorithm," *IEEE J. Emerg. Sel. Topics Power Electron.*, vol. 1, no. 2, pp. 104–113, Jun. 2013.

[144] B. Singh and S. R. Arya, "Implementation of single-phase enhanced phase-locked loop-based control algorithm for three-phase DSTATCOM," *IEEE Trans. Power Del.*, vol. 28, no. 3, pp. 1516–1524, Jul. 2013.

[145] B. Singh, S. K. Dube, and S. R. Arya, "Hyperbolic tangent function-based least mean-square control algorithm for distribution static compensator," *IET Gener., Transmiss. Distrib.*, vol. 8, no. 12, pp. 2102–2113, Dec. 2014.

[146] S. R. Arya, B. Singh, A. Chandra, and K. Al-Haddad, "Learning-based anti-Hebbian algorithm for control of distribution static compensator," *IEEE Trans. Ind. Electron.*, vol. 61, no. 11, pp. 6004–6012, Nov. 2014.

[147] B. Singh and S. R. Arya, "Back-propagation control algorithm for power quality improvement using DSTATCOM," *IEEE Trans. Ind. Electron.*, vol. 61, no. 3, pp. 1204–1212, Mar. 2014.

[148] B. Singh, S. R. Arya, A. Chandra, and K. Al-Haddad, "Implementation of adaptive filter in distribution static compensator," *IEEE Trans. Ind. Appl.*, vol. 50, no. 5, pp. 3026–3036, Sep. 2014.

[149] S. R. Arya and B. Singh, "Power quality improvement under nonideal AC mains in distribution system," *Electric Power Syst. Res.*, vol. 106, pp. 86–94, Jan. 2014.

[150] B. Singh, S. R. Arya, and K. Kant, "Notch filter-based fundamental frequency component extraction to control distribution static compensator for mitigating current-related power quality problems," *IET Power Electron.*, vol. 8, no. 9, pp. 1758–1766, Sep. 2015.

[151] S. R. Arya and B. Singh, "Implementation of kernel incremental metalearning algorithm in distribution static compensator," *IEEE Trans. Power Electron.*, vol. 30, no. 3, pp. 1157–1169, Mar. 2015.

[152] B. Singh, S. K. Dube, and S. R. Arya, "An improved control algorithm of DSTATCOM for power quality improvement," *Int. J. Electr. Power Energy Syst.*, vol. 64, pp. 493–504, Jan. 2015.

[153] S. Shukla, B. Singh, and S. Mishra, "Implementation of empirical mode decomposition for shunt active filter," in *Proc. IEEE IAS Joint Ind. Commercial Power Syst. Petroleum Chem. Ind. Conf. (ICPSPCIC)*, Nov. 2015, pp. 174–181.

[154] C. Jain and B. Singh, "Solar energy used for grid connection: A detailed assessment including frequency response and algorithm comparisons for an energy conversion system," *IEEE Ind. Appl. Mag.*, vol. 23, no. 2, pp. 37–50, Mar. 2017.

[155] R. Kumar Agarwal, I. Hussain, and B. Singh, "Three-phase single-stage grid tied solar PV ECS using PLL-less fast CTF control technique," *IET Power Electron.*, vol. 10, no. 2, pp. 178–188, Feb. 2017.

[156] A. S. Bubshait, A. Mortezaei, M. G. Simoes, and T. D. C. Busarello, "Power quality enhancement for a grid connected wind turbine energy system," *IEEE Trans. Ind. Appl.*, vol. 53, no. 3, pp. 2495–2505, Jun. 2017.

[157] R. S. R. Chilipi, N. Al Sayari, K. H. Al Hosani, and A. R. Beig, "Adaptive notch filter-based multipurpose control scheme for grid-interfaced three-phase four-wire DG inverter," *IEEE Trans. Ind. Appl.*, vol. 53, no. 4, pp. 4015–4027, Jul. 2017.

[158] N. Beniwal, I. Hussain, B. Singh, A. Chandra, and K. Al-Haddad, "Adaptive control scheme for three-phase four wire grid tied SPV system with DSTATCOM capabilities," in *Proc. Nat. Power Syst. Conf. (NPSC)*, Dec. 2016, pp. 1–6.

[159] B. Huang, Y. Xiao, J. Sun, and G. Wei, "A variable step-size FXLMS algorithm for narrowband active noise control," *IEEE Trans. Audio, Speech, Language Process.*, vol. 21, no. 2, pp. 301–312, Feb. 2013.

[160] Y. Han, L. Xu, M. M. Khan, G. Yao, L.-D. Zhou, and C. Chen, "A novel synchronization scheme for grid-connected converters by using adaptive linear optimal filter based PLL (ALOF PLL)," *Simul. Model. Pract. Theory*, vol. 17, no. 7, pp. 1299–1345, Aug. 2009.

[161] B. Singh, R. R. Chilipi, G. Bhuvaneswari, S. Madishetti, and S. S. Murthy, "Static synchronous compensator-variable frequency drive for voltage and frequency control of small-hydro driven self-excited induction generators system," *IET Gener., Transmiss. Distrib.*, vol. 8, no. 9, pp. 1528–1538, Sep. 2014.

[162] K. Reddy and B. Singh, "Dual mode multi-functional small hydro and SPV generation based reconfigurable system under non-ideal grid conditions," *IEEE Trans. Smart Grid*, vol. 9, no. 5, pp. 4942–4952, Sep. 2018.

[163] P. Garcia, C. A. Garcia, L. M. Fernandez, F. Llorens, and F. Jurado, "ANFIS-based control of a grid-connected hybrid system integrating renewable energies, hydrogen and batteries," *IEEE Trans. Ind. Informat.*, vol. 10, no. 2, pp. 1107–1117, May 2014.

[164] A. Kulkarni and V. John, "Mitigation of lower order harmonics in a grid-connected single-phase PV inverter," *IEEE Trans. Power Electron.*, vol. 28, no. 11, pp. 5024–5037, Nov. 2013.

[165] L. Liu, H. Li, Y. Xue, and W. Liu, "Reactive power compensation and optimization strategy for grid-interactive cascaded photovoltaic systems," *IEEE Trans. Power Electron.*, vol. 30, no. 1, pp. 188–202, Jan. 2015.

[166] T. K. Roy, M. A. Mahmud, A. M. T. Oo, and M. E. Haque, "Robust nonlinear adaptive backstepping controller design for three-phase grid-connected solar photovoltaic systems with unknown parameters," in *Proc. IEEE Power Energy Soc. Gen. Meeting (PESGM)*, Jul. 2016, pp. 1–5.

[167] A. Tilli and C. Conficoni, "Control of shunt active filters with actuation and current limits," *IEEE Trans. Control Syst. Technol.*, vol. 24, no. 2, pp. 644–653, Mar. 2016.

[168] C. Jain and B. Singh, "An adjustable DC link voltage-based control of multifunctional grid interfaced solar PV system," *IEEE J. Emerg. Sel. Topics Power Electron.*, vol. 5, no. 2, pp. 651–660, Jun. 2017.

[169] B. Singh, S. Kumar, and C. Jain, "Damped-SOGI-based control algorithm for solar PV power generating system," *IEEE Trans. Ind. Appl.*, vol. 53, no. 3, pp. 1780–1788, May 2017.

[170] B. Singh and C. Jain, "A decoupled adaptive noise detection based control approach for a grid supportive SPV system," *IEEE Trans. Ind. Appl.*, vol. 53, no. 5, pp. 4894–4902, Sep. 2017.

[171] G. S. Chawda and A. Gafoor Shaik, "Adaptive reactive power control of DSTATCOM in weak AC grid with high wind energy penetration," in *Proc. IEEE 16th India Council Int. Conf. (INDICON)*, Dec. 2019, pp. 1–4.

[172] M. Srinivas, I. Hussain, and B. Singh, "Combined LMS–LMF-based control algorithm of DSTATCOM for power quality enhancement in distribution system," *IEEE Trans. Ind. Electron.*, vol. 63, no. 7, pp. 4160–4168, Jul. 2016.
[173] A. K. Giri, S. R. Arya, and R. Maurya, "Compensation of power quality problems in wind-based renewable energy system for small consumer as isolated loads," *IEEE Trans. Ind. Electron.*, vol. 66, no. 11, pp. 9023–9031, Nov. 2019.
[174] B. Singh, C. Jain, and S. Goel, "ILST control algorithm of single-stage dual purpose grid connected solar PV system," *IEEE Trans. Power Electron.*, vol. 29, no. 10, pp. 5347–5357, Oct. 2014.
[175] B. Singh and S. R. Arya, "Adaptive theory-based improved linear sinusoidal tracer control algorithm for DSTATCOM," *IEEE Trans. Power Electron.*, vol. 28, no. 8, pp. 3768–3778, Aug. 2013.

GAJENDRA SINGH CHAWDA (Graduate Student Member, IEEE) was born in Mandsaur, India, in 1986. He received the Diploma degree in electrical engineering from the Government Polytechnic College, Jaora, India, in 2004, the B.E. degree in electrical and electronics engineering from Rajiv Gandhi Proudyogiki Vishwavidyalaya, Bhopal, India, in 2008, and the M.Tech. degree in electrical power system from NIT Kurukshetra, Haryana, India, in 2013. He is currently pursuing the Ph.D. degree with the Department of Electrical Engineering, IIT Jodhpur, India. His research interests include power electronics, power quality, custom power devices, renewable energy systems, and smart grid control.

ABDUL GAFOOR SHAIK (Member, IEEE) received the Ph.D. degree in power systems. He is an Associate Professor with the Department of Electrical Engineering, IIT Jodhpur. He has an industrial and academic research experience of more than 20 years. He has published over 50 research articles in reputed journals, international conferences, and book chapters. He has wide research experience in the area of power system protection and power quality. His research interests include the development of power system protection algorithms using multi-resolution analysis, such as wavelet transform and S-transform and power quality mitigation in distribution network with RE sources using adaptive control algorithms. The courses taught by him include power system protection, electrical machines, power system, power electronics, smart grid, and basic electrical engineering. He always excelled in academics and awarded a Gold Medal at graduate and post graduate levels. He was a recipient of the Best Paper Award from the Institution of Engineers India in 2015. His core team comprises of highly skilled students pursuing master's and Ph.D. degrees in the area of power quality, induction motor protection, power system protection, and smart grid.

OM PRAKASH MAHELA (Member, IEEE) received the B.E. degree from the College of Technology and Engineering, Udaipur, India, in 2002, the M.Tech. degree from Jagannath University, Jaipur, India, in 2013, and the Ph.D. degree from IIT Jodhpur, India, in 2018, all in electrical engineering. From 2002 to 2004, he was an Assistant Professor with the Rajasthan Institute of Engineering and Technology, Jaipur, India. From 2004 to 2014, he was a Junior Engineer with the Rajasthan Rajya Vidyut Prasaran Nigam Ltd., India and Assistant Engineer since July 2014. He has authored more than 130 research articles and book chapters. His research interests include power quality, power system planning, grid integration of renewable energy sources, FACTS devices, transmission line protection, and condition monitoring. He was a recipient of the University Rank Certificate in 2002, Gold Medal in 2013, the Best Research Paper Award in 2018, and C.V. Raman Gold Medal in 2019.

SANJEEVIKUMAR PADMANABAN (Senior Member, IEEE) received the bachelor's degree in electrical engineering from the University of Madras, Chennai, India, in 2002, the master's degree (Hons.) in electrical engineering from Pondicherry University, Puducherry, India, in 2006, and the Ph.D. degree in electrical engineering from the University of Bologna, Bologna, Italy, in 2012.

He was an Associate Professor with VIT University from 2012 to 2013. In 2013, he joined the National Institute of Technology, India, as a Faculty Member. In 2014, he was invited as a Visiting Researcher at the Department of Electrical Engineering, Qatar University, Doha, Qatar, funded by the Qatar National Research Foundation (Government of Qatar). He continued his research activities with the Dublin Institute of Technology, Dublin, Ireland, in 2014. He was an Associate Professor with the Department of Electrical and Electronics Engineering, University of Johannesburg, Johannesburg, South Africa, from 2016 to 2018. Since 2018, he has been a Faculty Member with the Department of Energy Technology, Aalborg University, Aalborg, Denmark. He has authored more than 300 scientific articles. He is a Fellow of the Institution of Engineers, India, the Institution of Electronics and Telecommunication Engineers, India, and the Institution of Engineering and Technology, U.K. He was a recipient of the Best Paper cum Most Excellence Research Paper Award from IET-SEISCON'13, IET-CEAT'16, IEEE-EECSI'19, IEEE-CENCON'19, and five best paper awards from ETAEERE'16 sponsored *Lecture Notes in Electrical Engineering* (Springer). He is an Editor/Associate Editor/Editorial Board for refereed journals, in particular the IEEE Systems Journal, the IEEE Transactions on Industry Applications, IEEE Access, *IET Power Electronics*, and *International Transactions on Electrical Energy Systems* (Wiley), and the Subject Editor of the *IET Renewable Power Generation*, *IET Generation, Transmission, and Distribution*, and *FACTS* journal (Canada).

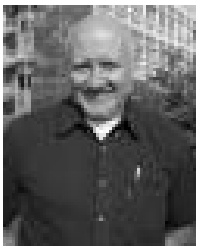

JENS BO HOLM-NIELSEN (Senior Member, IEEE) received the M.Sc. degree in agricultural systems, crops, and soil science from Royal Veterinary and Agricultural University (KVL), Copenhagen, Denmark, in 1980, and the Ph.D. degree in process analytical technologies for biogas systems from Aalborg University, Aalborg, Denmark, in 2008. He is currently with the Department of Energy Technology, Aalborg University, and the Head of the Esbjerg Energy Section. He is the Head of the Research Group, Center for Bioenergy and Green Engineering, established in 2009. He has vast experience in the field of biorefinery concepts and biogas production–anaerobic digestion. He has implemented projects of bioenergy systems in Denmark with provinces and European states. He was the Technical Advisor for many industries in this field. He has executed many large-scale European Union and United Nations projects in research aspects of bioenergy, biorefinery processes, and the full chain of biogas and green engineering. He has authored more than 300 scientific articles. His current research interests include renewable energy, sustainability, and green jobs for all. He was a member on invitation with various capacities in the committee for over 500 various international conferences and an organizer of international conferences, workshops, and training programs in Europe, Central Asia, and China.